Charge-Transfer Salts of Ferrocene Derivatives with Bis(maleonitriledithiolato)metallate(III) Complexes ($[M(mnt)_2]^-$, M = Ni, Pt): A Ground-State High-Spin $[(Ni(mnt)_2)_2]^{2-}$ Dimer

by **Stefan Zürcher**, **Jeannine Petrig**, **Mauro Perseghini**, **Volker Gramlich**, **Michael Wörle**, **Dieter von Arx**, and **Antonio Togni***

Laboratory of Inorganic Chemistry, ETH Zentrum, Swiss Federal Institute of Technology, CH-8092 Zürich, Tel: 01 632 22 36, Fax: 01 632 10 90, e-mail: togni@inorg.chem.ethz.ch

New hexamethylated ferrocene derivatives containing thioether moieties (1,1′-bis[(*tert*-butyl)thio]-2,2′,3,3′,4,4′-hexamethylferrocene (**3a**,**b**)) or fused S-heteropolycyclic substituents (*rac*-1-[(1,3-benzodithiol-2-yliden)methyl]-2,2′,3,3′,4,4′-hexamethylferrocene (**5**) and *rac*-1-[1,2-bis(1,3-benzodithiol-2-yliden)ethyl]-2,2′,3,3′,4,4′-hexamethylferrocene (**14**)), as well as a series of ferrocene-substituted vinylogous tetrathiafulvalenes (1,1′-bis[1,2-bis(1,3-benzodithiol-2-yliden)ethyl]ferrocene (**6a**), 1,1′-bis[1-(1,3-benzodithiol-2-yliden)-2-(5,6-dihydro-1,3-dithiolo[4,5-*b*][1,4]dithiin-2-yliden)ethyl]ferrocene (**6b**), [1,2-bis(1,3-benzodithiol-2-yliden)-ethyl]ferrocene (**21a**), [1-(1,3-benzodithiol-2-yliden)-2-(5,6-dihydro-1,3-dithiolo[4,5-*b*][1,4]dithiin-2-yliden)-ethyl]ferrocene (**21b**), [1,2-bis(5,6-dihydro-1,3-dithiolo[4,5-*b*][1,4]dithiin-2-yliden)ethyl]ferrocene (**21c**), [1-(5,6-dihydro-1,3-dithiolo[4,5-*b*][1,4]dithiin-2-yliden)-2-(1,3-benzodithiol-2-yliden)ethyl]ferrocene (**21d**)) were prepared and fully characterized. Their redox properties show that some of them are easily oxidized and undergo transformation to paramagnetic salts containing bis(maleonitriledithiolato)-metallate(III) anions $[M(mnt)_2]^-$ (M = Ni, Pt; bis[2,3-dimercapto-κS)but-2-enedinitrilato(2^-)]nickelate (1^-) or -platinate (1^-). The derivatives [**3a**][$Ni(mnt)_2$] (**26**), [**3a**][$Pt(mnt)_2$] (**27**), [Fe{(η^5-$C_5Me_4S)_2$S}][$Ni(Mnt)_2$] (**28**), [Fe{(η^5-$C_5Me_4S)_2$S}][$Pt(mnt)_2$] (**29**), [**5**] [$Ni(mnt)_2$]·$ClCH_2CH_2Cl$ (**30**), [**6a**] [$Ni(mnt)_2$] (**31**), [**6a**] [$Ni(mnt)_2$]·$ClCH_2CH_2Cl$ (**31a**), [**6a**] [$Pt(mnt)_2$] [**32**], and [**6b**] [$Ni(mnt)_2$] (**33**) were prepared and fully characterized, including by SQUID (superconducting quantum interference device) susceptibility measurements. X-Ray crystal-structural studies of the neutral ferrocene derivatives **6a**,**b**, **21c**,**d**, and 1,1′-bis[1-(1,3-benzodithiol-2-yliden)-2-oxoethyl]ferrocene (**23**), as well as of the charge-transfer salts **26**–**28**, **30**, and **31a**, are reported. The salts **28** and **30** display both a $D^+A^-A^-D^+$ structural motif, however, with a different relative arrangement of the $[\{Ni(mnt)_2\}_2]^{2-}$ dimers, thus giving rise to different but strong antiferromagnetic couplings. Salt **26** exhibits isolated ferromagnetically coupled $[\{Ni(mnt)_2\}_2]^{2-}$ dimers. Salt **27** displays a $D^+A^-D^+A^-$ structural motif in all three space dimensions, and a week ferromagnetic ordering at low temperature. Salt **31a**, on the contrary, shows segregated stacks of cations and anions. The cations are connected with each other in two dimensions, and the anions are separated by a 1,2-dichloroethane molecule.

1. Introduction. – We recently reported synthesis and characterization of bis(maleonitriledithiolato)metallate(III) salts $[M(mnt)_2]^-$ (M = Ni, Co, Pt; bis[2,3-di(mercapto-κS)-but-2-enedinitrilato(2−)]metallate(2−)) with the octamethylferrocenyl thioethers [1] **1** and **2**, as well as with ferrocenes containing S-heterocycles [2–3] related to the basic tetrathiafulvalene (TTF) structure. These compounds were shown to display weak ferromagnetic or antiferromagnetic interactions. The physical properties of such materials strongly depend on the relative arrangement of cations and anions in the solid state. In turn, the three-dimensional structure is influenced by the nature and size of the S-containing substituents on the ferrocene. In continuation of these investigations concerning charge-transfer (CT) complexes with ferrocene electron

donors [1–7], a series of bis(maleonitriledithiolato)nickelate and -platinate complexes with a variety of new ferrocenes (see **3**–**6**) were prepared. The aim of the present study was to further explore how subtle changes at the electron-donor molecular level influence the material properties of the corresponding CT complexes. Thus, the present work was conducted on two main lines. First, in the ferrocenyl thioether series, the new hexamethyl derivatives **3** and **4** were prepared, thus allowing a comparison with their octamethyl counterparts. Can such a minor structural change significantly alter the properties of the corresponding CT complexes? Second, a more drastic modification of the benzodithiol-containing derivatives, *i.e.*, towards branched compounds comprising up to four heterocyclic units (see **6**), could lead to multiple intermolecular interactions in the solid state.

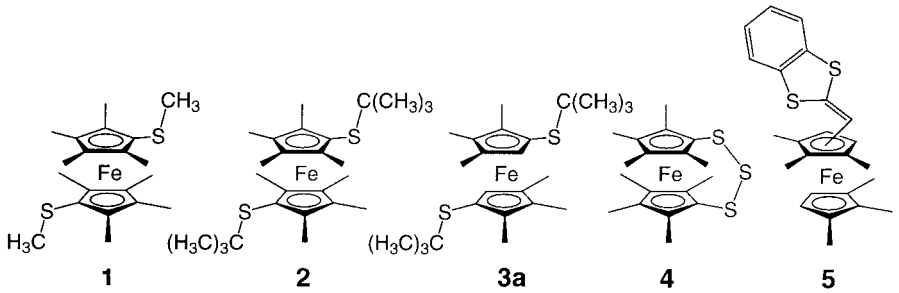

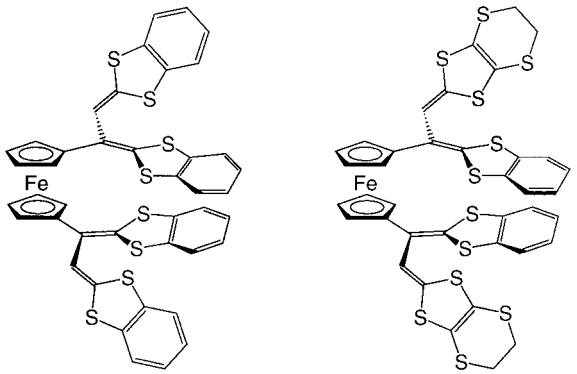

2. Results and Discussion. – 2.1. *Synthesis of Ferrocene Derivatives as Electron Donors.* 2.1.1. *Hexamethylated Ferrocenes.* As opposed to tetramethylcyclo-penta-1,3-diene, 1,2,3-trimethylcyclopenta-1,3-diene (**10**) is not stable and dimerizes slowly at room temperature and upon distillation. Because the *retro-Diels-Alder* reaction of dimeric **10** does not occur as easily as for dicyclopentadiene, this compound is more difficult to access [8][9]. However, **10** may be obtained by distillation of trimethylcyclopent-2-en-1-ols (**9**) at atmospheric pressure and at 170° and has to be used directly, after removal of the co-distilled water with sodium sulfate. Thus, for the synthesis of 1,1′-bis[(*tert*-butyl)thio]-2,2′,3,3′,4,4′-hexamethylferrocene (**3**), a strategy for the direct conversion of trimethylcyclopentenone **7** to the S-substituted ligand **8** was needed. As

illustrated in *Scheme 1*, **8** was obtained in moderate yields applying a reported method [10][11]. The synthesis of the corresponding ferrocenes **3** was then achieved analogously to that of the octamethylated counterparts [1]. The product obtained was a 1:1 mixture of two diastereoisomers, *i.e.*, an achiral *meso*-form **3a** and a pair of enantiomers **3b** that could be distinguished by NMR spectroscopy. In particular, the cyclopenta-2,4-dien-1-yl (Cp) protons of **3a** and **3b** show distinctly different chemical shifts in the ^{1}H-NMR spectrum. Upon recrystallization from hexane, an enriched sample (diastereoisomer ratio of 85:15) was obtained. However, the configurational assignment of the diastereoisomers could be made only *via* an X-ray crystallographic study of the corresponding CT [Ni(mnt)$_2$] salt (*vide infra*) obtained from the enriched mixture. This revealed that the enriched component is the *meso*-form **3a**, thus making a complete assignment of the ^{1}H-NMR spectra of the two compounds possible. Reduction of the [Ni(mnt)$_2$] salt with sodium dithionite afforded the ferrocene **3a** quantitatively, and contaminated with only 6% of **3b**.

Scheme 1

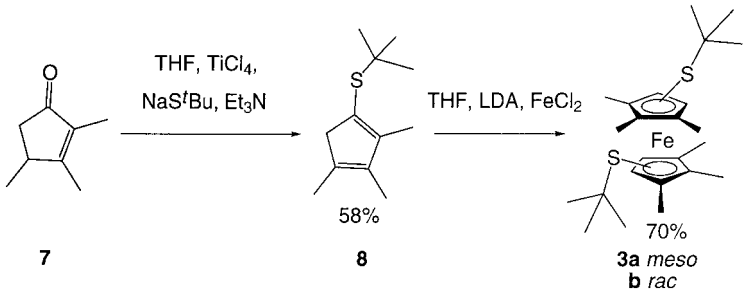

The 1,1′,2,2′,3,3′-hexamethylferrocene (**11**) was needed as a starting material for the preparation of the corresponding mono- and dialdehydes, intermediates in the synthesis of donor molecules containing fused S-heterocycles such as, *e.g.*, **5** [2–4][6][12]. As opposed to what was observed for the octamethylated derivatives previously reported from our laboratory [4][6], it was anticipated that the S-heterocycles in the hexamethylated series would assume an orientation coplanar with the Cp ring and, therefore, be in conjugation with the ferrocene. Hexamethylferrocene **11** was obtained in moderate yield from crude **10** as shown in *Scheme 2*. The dilithiation of **11**, but not of the corresponding octamethyl derivative, with butyllithium (BuLi) in the presence of *N*,*N*,*N*′,*N*′-tetramethylethylenediamine (TMEDA) appears to be possible. However, the followup products upon reaction with DMF and sulfur, respectively, *i.e.*, the dialdehyde **15** and the trithioferrocene **16**, could be isolated in yields of a few percent only. Even the use of stronger bases such as *tert*-butyllithium or 'Lickor' [13] did not improve these preparations. Further work with **15** and **16** was, therefore, discontinued. On the other hand, monosubstitution of **11** could be achieved more easily. Thus, the monoaldehyde **12** was prepared *via* a *Vilsmeier* reaction, as in the case of the octamethylated derivative [14–16]. The following *Wittig-Horner* reaction afforded the new ferrocene donor **5** in good yield. In an attempt to further formylate **5** under *Vilsmeier* conditions, we found a selective functionalization of the olefinic C–H bond, and not at the second Cp ring. This reaction opens the possibility to

prepare a new class of donor molecules belonging to the class of vinylogous tetrathiafulvalenes [17–26]. Indeed, aldehyde **13** reacted in an additional *Wittig-Horner* reaction to give the new donor **14**. Finally, one should note that compounds **5** and **12**–**14** are chiral and that they were obtained as racemates.

Scheme 2

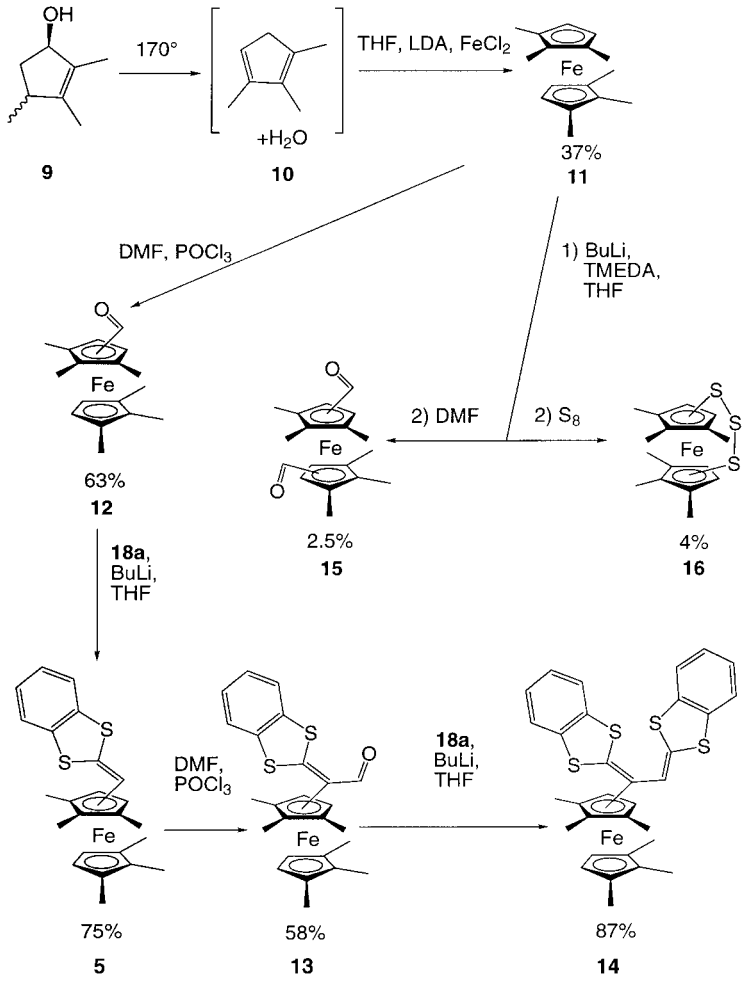

2.1.2. *Ferrocenes Containing Vinylogous Tetrathiafulvalenes.* The formylation reaction described above prompted us to prepare a series of vinylogous TTF compounds based on non-methylated ferrocene, for which the accessibility of mono- and 1,1′-disubstituted derivatives was known [2]. Thus, the monosubstituted ferrocenes **19a** and **19b** were prepared in very good yields from **17** and **18a** or **18b**, respectively (*Scheme 3*). As expected, these compounds could be selectively converted under *Vilsmeier* conditions to the aldehydes **20a** and **20b**, respectively, in high yields. However, aldehyde **20b** required the reagent oxalyl chloride instead of phosphoric

trichloride, which gave no detectable product. From the intermediates **20a**,**b**, the four vinylogous ferrocenyl tetrathiafulvalenes **21a**–**d** were prepared in moderate to good yields by *Wittig-Horner* reactions.

Scheme 3

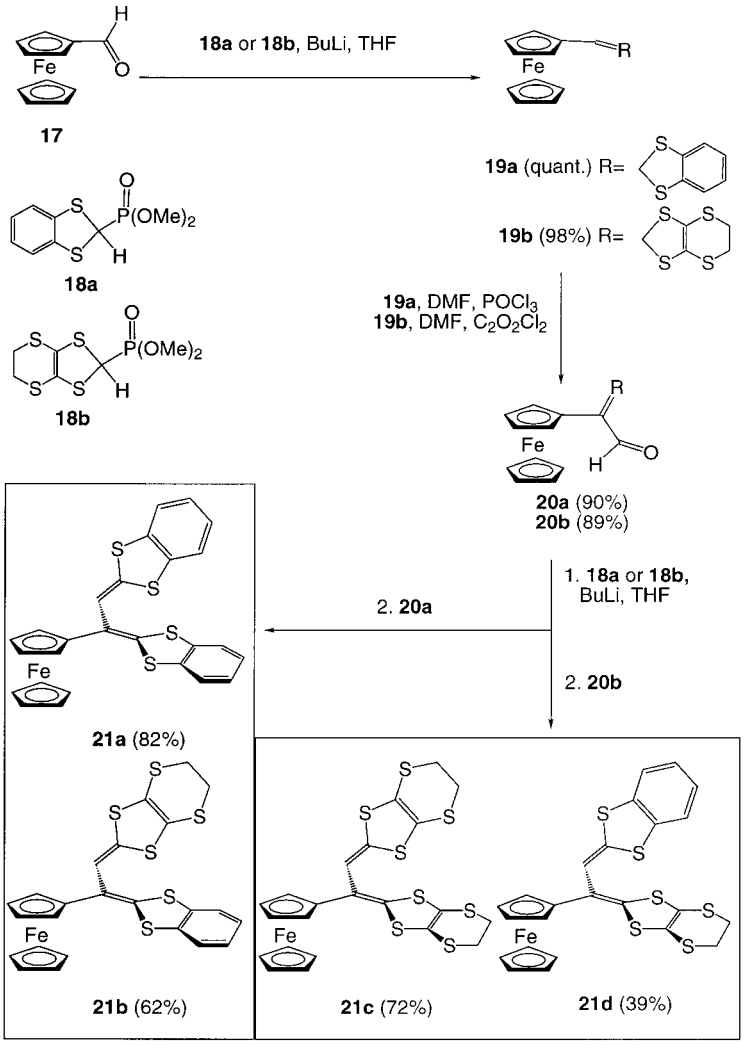

Finally, from the known precursor **22a**, the ferrocene derivatives **6a** and **6b** containing two vinylogous tetrathiafulvalenes were obtained in good yields *via* **23** (*Scheme 4*). In contrast, **22b** did not react under the same conditions as **22a**, neither with oxalyl chloride nor with phosphoric trichloride. It appears that ferrocene oxidation of **22b** prevails under these conditions, as indicated by the green color of the reaction mixture.

Scheme 4

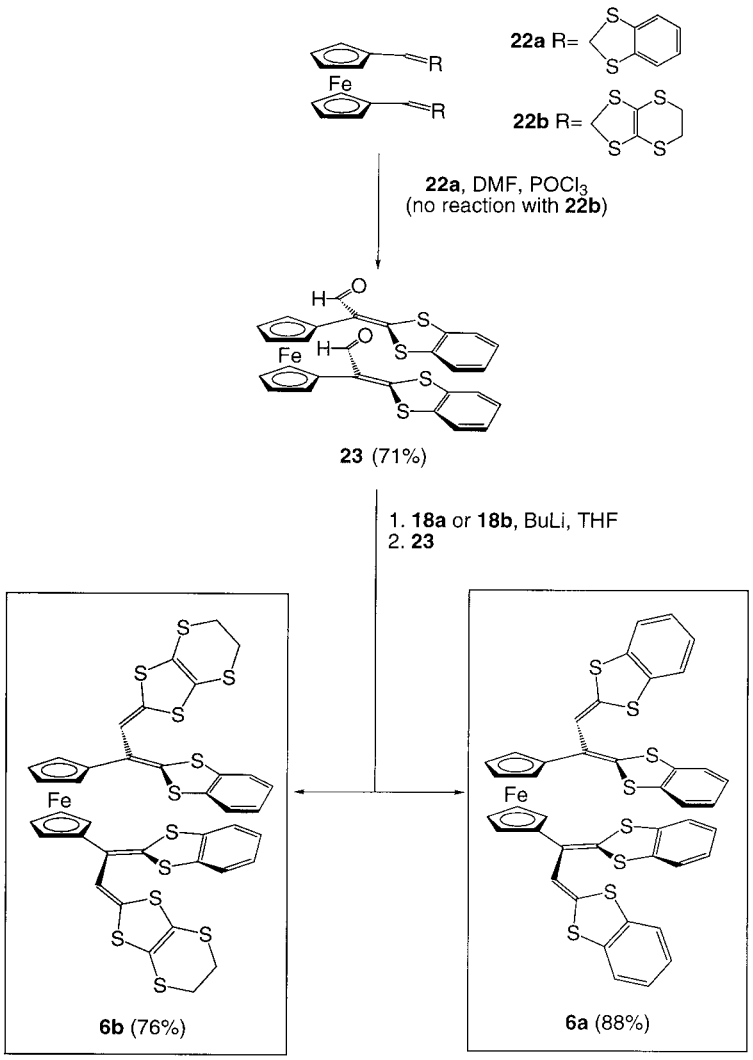

2.1.3. *Synthesis of Charge-Transfer Complexes* **26**–**33**. The preparation of $[M(mnt)_2]^-$ salts **26**–**33** (M = Ni, Pt) containing the donors **3**–**6** was achieved according to the published procedure by reaction with the ferrocenium bis(maleonitriledithiolato)metallates **24** or **25** (see *Scheme 5*) [1][3]. With the new ferrocene-bridged, vinylogous bis(tetrathiafulvalene) **6a** and $[Ni(mnt)_2]^-$ salt **24**, two different products **31** and **31a** were obtained in ratios close to 1 : 1 from dichloroethane solutions. One of them, **31a**, is the dichloroethane adduct which crystallized in nice prismatic plates, whereas the second one, **31**, is the solvent-free 1 : 1 salt, obtained as extremly thin needles. The $[Pt(mnt)_2]^-$ salt **32** of **6a** and the $[Ni(mnt)_2]^-$ salt **33** of **6b** could be isolated in only moderate yields. All new $[M(mnt)_2]^-$ salts described in this study

display sharp $\tilde{\nu}$(CN) bands in the narrow range between 2205 and 2209 cm^{-1}. This is also true for the starting monoanionic forms $(Et_4N)[M(mnt]_2]$. The IR opacity of the dichloroethane adduct **31a** down to 3000 cm^{-1} is indicative of a semiconductor-like behavior of this compound.

Scheme 5

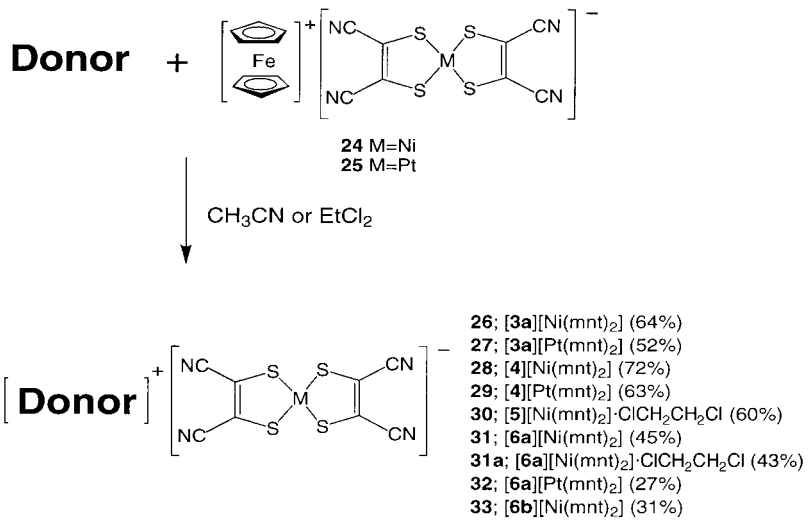

2.2. *Cyclovoltammetric Measurements.* Routine cyclovoltammetric measurements in CH_2Cl_2 solution were carried out for all new ferrocene compounds, to check their ability to form CT complexes. Redox potentials are reported in *Table 1*. The ferrocenes **3a**,**b**, **5**, **6a**,**b**, **11**, **12**, **15**, and **16** all show one reversible one-electron oxidation. The redox potential increases by *ca.* 0.3 V per aldehyde group, and *ca.* 0.1 V per thioether group, as compared to the corresponding non-substituted derivatives.

The two donors **5** and **14** show two reversible oxidation waves. The lower one concerns the ferrocene unit, whereas the second process corresponds to an oxidation of the S-substituent. Cyclovoltammograms for the three compounds **5**, **13**, and **14** are depicted in *Fig. 1*. The two one-electron processes in **5** are separated by 0.78 V (*Table 1*). In **14**, the oxidation of the ferrocene occurs at a slightly higher potential than in **5**. This can be explained by the larger steric hindrance of the substituent on **14**, such that a coplanar geometry with the Cp ring is no longer possible, thus reducing the delocalization of the positive charge on the substituent. The second oxidation step, which is a reversible two-electron oxidation, is lowered by 0.14 V, as compared to **5**. Thus the two potentials are separated by only 0.61 V. The aldehyde group of **13** increases the redox potential of the ferrocene by 0.13 V. This is much less than the effect of an aldehyde group directly attached to the Cp ring. Moreover, **13** shows a second irreversible oxidation at a potential of $+1.09$ V.

Table 1. *Formal Electrode Potentials* (*vs.* Fc/Fc^+) *for Ferrocene Derivatives in Dichloromethane Solution*[a])

Compound (reduced form)	$E^{\circ\prime}_{(0\rightarrow n+)}$ [V]	ΔE_p [mV]	i_{pc}/i_{pa}	$E^{\circ\prime}_{(n+\rightarrow m+)}$ [V]	ΔE_p [mV]	i_{pc}/i_{pa}
3a,**b**	$-0.19^{b})_{(0\rightarrow1)}$	104	0.95			
4	$-0.10^{c})_{(0\rightarrow1)}$	272	1.00			
5	$-0.35^{c})_{(0\rightarrow1)}$	132	0.96	$+0.43^{c})_{(1\rightarrow2)}$	140	1.13
6a	$-0.16^{c})_{(0\rightarrow1)}$	106	1.05	$(+0.24)^{b})_{(1\rightarrow2)}$		
				$(+0.33)^{b})_{(2\rightarrow3)}$		
				$(+0.70)^{b})_{(3\rightarrow4)}$		
				$(+0.80)^{b}{}_{(4\rightarrow5)}$		
				$(+0.37)^{b})_{(5\rightarrow3)}$VIIb[e])		
				$(+0.04)^{b})_{(3\rightarrow1)}$VIIa[e])		
				$(+0.14)^{c})_{(3\rightarrow1)}$		
6b	$-0.16^{d})_{(0\rightarrow1)}$	98	1.8	$(+0.13)^{d})_{(1\rightarrow2)}$		
				$(+0.21)^{d})_{(2\rightarrow3)}$		
				$+0.57^{d})_{(3\rightarrow4)}$VIa[e])	224	
				$(-0.03)^{d})_{(3\rightarrow1)}$VIb[e])		
				$(+0.05)^{b})_{(3\rightarrow1)}$		
11	$-0.34^{b})_{(0\rightarrow1)}$	404	0.96			
12	$-0.03^{c})_{(0\rightarrow1)}$	120	0.97			
13	$-0.22^{c})_{(0\rightarrow1)}$	205	1.39	$(+1.09)^{b})_{(1\rightarrow2)}$		
14	$-0.32^{c})_{(0\rightarrow1)}$	136	1.02	$+0.29^{c})_{(1\rightarrow2)}$	164	0.97
15	$+0.23^{b})_{(0\rightarrow1)}$	92	0.94			
16	$-0.03^{c})_{(0\rightarrow1)}$	112	0.98			
19a	$-0.07^{b})_{(0\rightarrow1)}$	110	0.69	$+0.455^{b})_{(1\rightarrow2)}$	119	0.31
19b	$-0.08^{c})_{(0\rightarrow1)}$	96	0.88	$+0.30^{c})_{(1\rightarrow2)}$	192	1.6
20a	$+0.04^{c})_{(0\rightarrow1)}$	58	0.97	$(+0.78)^{b})_{(1\rightarrow2)}$		
20b	$+0.03^{b})_{(0\rightarrow1)}$	200	0.81	$(+0.84)^{b})_{(1\rightarrow2)}$		
21a	$-0.08^{b})_{(0\rightarrow1)}$	98	0.96	$+0.20^{b})_{(1\rightarrow2)}$	86	
				$+0.36^{b})_{(2\rightarrow3)}$	166	
21b	$-0.07^{b})_{(0\rightarrow1)}$	107		$+0.13^{b})_{(1\rightarrow2)}$	56	
				$+0.34^{b})_{(2\rightarrow3)}$	118	
21c	$-0.10^{c})_{(0\rightarrow1)}$	90		$+0.08^{c})_{(1\rightarrow2)}$	90	
				$+0.34^{c})_{(2\rightarrow3)}$	130	
21d	$-0.10^{c})_{(0\rightarrow1)}$	137		$+0.14^{c})_{(1\rightarrow2)}$	138	
				$+0.35^{c})_{(2\rightarrow3)}$	168	
23	$+0.02^{b})_{(0\rightarrow1)}$	102	0.97	$(+0.78)^{b})_{(1\rightarrow2)}$		

[a]) All experiments were carried out in dry CH_2Cl_2/0.1M $(Bu_4N)BF_4$ *vs.* 0.05M Fc/Fc^+ reference electrode with $E^{\circ\prime} = +0.042$ V for ferrocene, and a Pt working electrode (all values are corrected for 0 V). Values in brackets are E_{pa} or E_{pc} (anodic or cathodic peak potentials), assigned only to irreversible oxidation steps. ΔE_p is the difference between E_{pa} and E_{pc} and i_{pc}/i_{pa} is the ratio between cathodic and anodic current indicative of the reversibility of the redox process. [b]) Scan rate 100 mV/s. [c]) Scan rate 20 mV/s. [d]) Scan rate 50 mV/s). [e]) See *Fig. 3* for peak identification.

The two mono-substituted ferrocenes **19a** and **19b** can both be oxidized twice. The first one-electron oxidation again is probably located on the ferrocene moiety, whereas the second corresponds to an electron removal from the substituent [2][6]. The potential of the first oxidation is *ca.* 100 mV higher than in the doubly substituted analogues. The two oxidation steps are not completely reversible, as shown by the ratio of the anodic and cathodic currents of 0.31 and 1.6, respectively (*Table 1*).

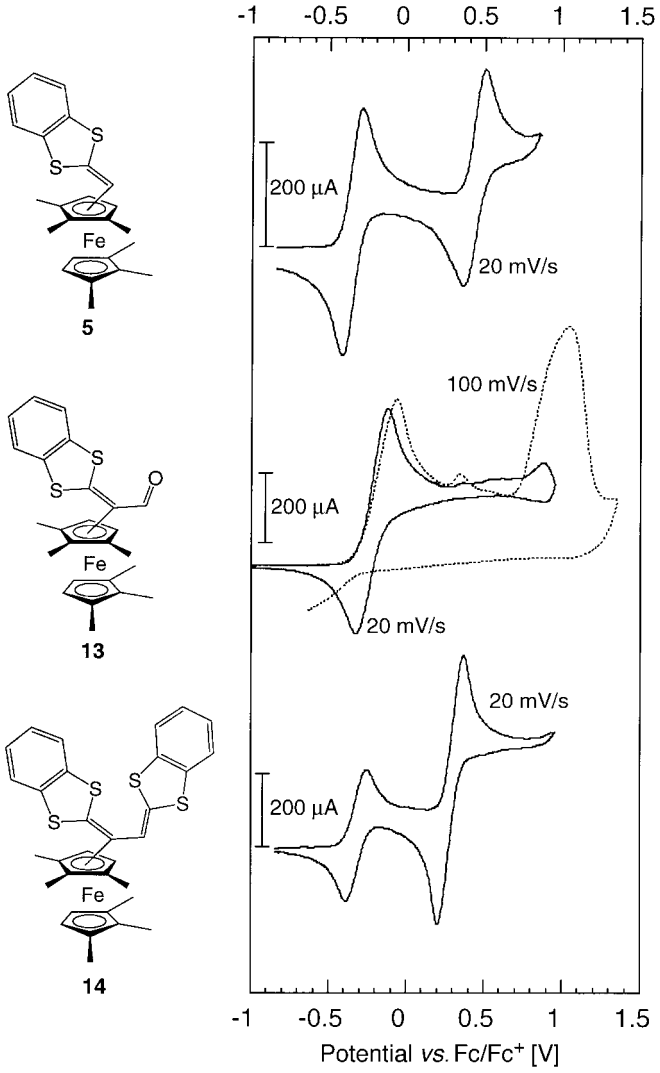

Fig. 1. *Cyclovoltammograms of the three ferrocene donors* **5**, **13**, *and* **14**

Both aldehydes **20a** and **20b** can be reversibly oxidized at a potential of +0.04 and +0.03 V, respectively (*Table 1*). Here again, the potentials increase by *ca.* 110 mV with respect to that of the precursors because of the acceptor group. At a potential of +0.78 and +0.84 V, respectively, a second irreversible oxidation occurs similarly to what is observed for the aldehydes **13** and **23**. The latter can be reversibly oxidized at a potential of +0.02 V, and an irreversible oxidation occurs at +0.78 V (see below, *Fig. 3*).

The four vinylogous tetrathiafulvalenes **21a**–**d** show three oxidation waves (*Fig. 2*). Because the three waves are overlapping, the ratios of the anodic and cathodic currents could not be determined. However, since the cycles overall are closed, probably no

decomposition of the compounds occurs. In all four cases, the reduction wave at the highest potential is very steep, and the corresponding current is higher than expected for a normal one-electron reduction step. Such effects can be detected when a conducting species precipitates at the electrode. Such behavior has been reported, for example, for $[Ni(dmit)_2]$ derivatives [27] ($dmit^{2-}$ = 1,3-dithiol-2-thione-4,5-dithiolato = 4,5-di(mercapto-κS)-1,3-dithiol-2-thione).

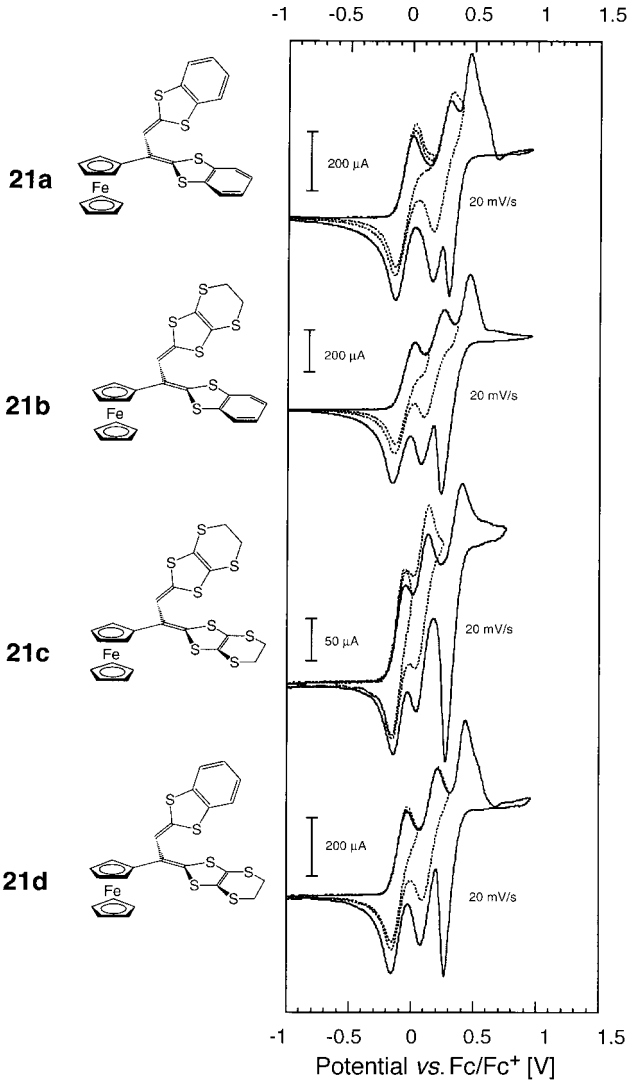

Fig. 2. *Cyclovoltammograms of the four vinylogous TTF derivatives* **21a–d**

Donor **6a** displays an interesting redox behavior (see *Fig. 3*), as it is possible to oxidize this compound in five descrete one-electron steps (steps I–V). However, the waves corresponding to the oxidations from $\mathbf{6a}^{1+}$ to $\mathbf{6a}^{3+}$ (steps II and III) and from $\mathbf{6a}^{3+}$

Table 2. *Experimental Data for the X-Ray Diffraction Studies of* **6a**,**b**, **21c**,**d**, **23**, **26**–**28**, **30**, *and* **31a**

	6a	**6b**	**21c**	**21d**	**23**
Empirical formula	$C_{42}H_{26}FeS_8$	$C_{40}H_{30}Cl_4FeS_{12}$	$C_{22}H_{18}FeS_8$	$C_{24}H_{28}FeS_6$	$C_{28}H_{18}FeO_2S_4$
M_r	843.00	1093.01	594.76	554.62	570.51
Crystal size/mm	$0.57 \times 0.27 \times 0.19$	$0.3 \times 0.3 \times 0.06$	$0.1 \times 0.02 \times 0.02$	$0.2 \times 0.1 \times 0.1$	$0.7 \times 0.3 \times 0.3$
Crystal system	triclinic	triclinic	orthorhombic	orthorhombic	monoclinic
Space group (No.)	$P\bar{1}$ (2)	$P\bar{1}$ (2)	$P2_12_12_1$ (19)	$P2_12_12_1$ (19)	$P2_1/c$ (14)
Temp.	room temp.	room temp.	room temp.	room temp.	room temp.
a/Å	14.170(3)	10.327(5)	11.799(10)	11.7920(3)	12.804(5)
b/Å	14.364(3)	13.002(7)	12.869(7)	12.9689(4)	14.716(6)
c/Å	20.603(4)	17.059(9)	15.478(12)	15.1203(4)	13.443(6)
α/deg	99.33(3)	90.70(2)	90	90	90
β/deg	106.27(3)	98.84(2)	90	90	111.42(3)
γ/deg	109.52(3)	98.43(2)	90	90	90
V/Å^3	3639.5(13)	2238(2)	2350(3)	2312.34(11)	2358(2)
Z	4	2	4	4	4
ρ(calc.)/g cm^{-3}	1.538	1.622	1.681	1.593	1.607
μ/mm^{-1}	0.906	10.388	1.363	1.206	1.021
Diffractometer	*Stoe image plate diffraction system*	*Picker Stoe*	*Syntex P21*	*Siemens Smart Platform with CCD detector*	*Syntex P21*
Wavelength λ/Å	MoK_α, $\lambda = 0.71073$	CuK_α, $\lambda = 1.54178$	MoK_α, $\lambda = 0.71073$	MoK_α, $\lambda = 0.71073$	MoK_α, $\lambda = 0.71073$
θ Range/deg	3.96–24.71	1.31–25.00	2.06–20.03	2.07–32.89	2.14–20.04
Measured reflections	21561	4601	1281	7850	2203
Observed reflections (n)[a]	10865	4601	1281	7850	2203
Parameters refined (p)	919	523	281	255	316
Abs. correction	none	integration	integration	empirical	integration
μ, max/min trans.		0.581/0.111	0.652/0.590	(SADABS)	0.774/0.717
wR_2 ($I > 2\sigma(I)$[b])	0.1139	0.1515	0.0513	0.0656	0.0620
R_1 ($I > 2\sigma(I)$[c])	0.0480	0.0530	0.0198	0.0341	0.0232
G.o.f. on $F^\wedge 2$[d])	1.022	1.046	1.012	0.889	1.062
Res. electron density eÅ^{-3}	0.564	0.731	0.160	0.234	0.164

to **6a**$^{5+}$ (steps IV and V) strongly overlap. Furthermore, the reduction part of the cycle shows only three waves, where two two-electron reductions (steps VI and VIIb) and one one-electron reduction (step VIIIb) can be detected. A two-electron reduction wave is observed also deriving from cation **6a**$^{3+}$ (VIIa), however at a peak potential higher by *ca*. 100 mV, as compared to the potential of the corresponding step (VIIb) observed in the full cycle. As in the case of the monosubstituted analogues **21a**–**d**, the closed redox cycles indicate that no compound degradation is occurring.

2.3. *Solid-State Structure of Neutral Donor Molecules and Charge-Transfer Salts.* 2.3.1. *Preamble.* Single-crystal X-ray diffraction studies were carried out for the five neutral ferrocene derivatives **23**, **6a**,**b**, and **21c**,**d**, and the five CT salts **26**–**28**, **30**, and **31a**. *Table 2* gives the relevant crystal and data-collection parameters. Bond distances and angles of each asymmetric unit were found to fall in the expected ranges and shall, therefore, not be discussed in detail. It was mainly of interest to see how the geometry and orientation of the substituents on the ferrocenes-moiety change in going from the

Table 2. (*cont.*)

	26	**27**	**28**	**30**	**31a**
Empirical formula	$C_{32}H_{28}FeN_4NiS_6$	$C_{32}H_{38}FeN_4PtS_6$	$C_{26}H_{24}FeN_4NiS_7$	$C_{34}H_{30}Cl_2FeN_4NiS_6$	$C_{52}H_{30}Cl_2FeN_4NiS_{12}$
M_r	785.59	921.96	731.48	872.44	1281.02
Crystal dimens/mm	$0.3 \times 0.24 \times 0.16$	$0.2 \times 0.2 \times 0.2$	$0.4 \times 0.3 \times 0.25$	$0.4 \times 0.25 \times 0.04$	$0.6 \times 0.4 \times 0.2$
Crystal system	monoclinic	orthorhombic	monoclinic	triclinic	monoclinic
Space group (No.)	$P2_1/n$ (14)	*Pbca* (61)	$P2_1/c$ (14)	$P\bar{1}$ (2)	$C2/c$ (15)
Temp.	room temp.	room temp.	room temp.	room temp.	room temp.
a/Å	12.48290(10)	13.297(39)	9.804(5)	9.537(5)	8.309(4)
b/Å	16.9929(3)	16.849(5)	11.392(8)	11.120(6)	23.202(12)
c/Å	18.54960(19)	17.301(9)	27.96(2)	18.691(9)	27.982(14)
α/deg	90	90	90	83.39(4)	90
β/deg	102.4630(10)	90	93.89(6)	77.83(3)	94.52
γ/deg	90	90	90	75.46(49)	90
V/Å^3	3842.03	3876(3)	3116	1872(2)	5378
Z	4	4	4	2	4
ρ(calc.)/g cm^{-3}	1.358	1.580	1.559	1.548	1.582
μ/mm^{-1}	1.220	4.329	1.563	8.424	8.202
Diffractometer	*Siemens Smart Platform* with *CCD* detector	*Syntex P21*	*Syntex P21*	*Picker Stoe*	*Picker Stoe*
Wavelength λ/Å	MoK_α, $\lambda = 0.71073$	MoK_α, $\lambda = 0.71073$	MoK_α, $\lambda = 0.71073$	CuK_α, $\lambda = 1.54178$	CuK_α, $\lambda = 1.54178$
θ Range/deg	1.64 – 21.98	2.28 – 20.04	1.93 – 17.53	1.21 – 25.00	1.59 – 25.00
Measured reflections	4685	1819	2164	3845	2772
Observed reflections	4685	1819	1990	3845	2772
Parameters refined (p)	399	209	371	433	327
Abs. correction	empirical	none	empirical	integration	integration
μ, max/min trans.	(SADABS)		(ψ scan)	0.712/0.173	0.207/0.061
wR_2 ($I > 2\sigma(I)$[b])	0.0954	0.0480	0.0676	0.1436	0.1346
R_1 ($I > 2\sigma(I)$[c])	0.0433	0.0221	0.0315	0.0554	0.0507
G.o.f. on $F^\wedge 2$[d])	1.043	0.689	0.889	1.049	1.130
Res. electron density eÅ^{-3}	0.366	0.509	0.407	0.856	0.435

[a]) ($|F_o^2| > 4.0\sigma(|F|^2)$). [b]) $wR_2 = [\sigma(w(F_o^2 - F_c^2)^2]/\sigma[w(F_o^2)^2]^{1/2}$. [c]) $R_1 = \sigma||F_o| - |F_c||/\sigma|F_o|$. [d]) G.o.f. $= S = [\sigma\,(w(F_o^2 - F_c^2)^2]/(n-p)]^{1/2}$.

neutral to the oxidized form, and how the arrangement of these groups influences the ordering of the anions.

2.3.2. *Neutral Donor Molecules.* First, it is important to note that the vinylogous TTF fragment seems to be very flexible, such that weak packing forces have a strong influence on its conformation. Thus, in all measured structures, except for the isomorphous **21c** and **21d**, the relative arrangement of this fragment is different, although ^{1}H-NMR spectra in solution indicate free rotation of these substituents.

The dialdehyde **23** crystallizes in the monoclinic space group $P2_1/c$, and a view of the molecule is shown in *Fig. 4*. The two Cp rings are almost parallel (interplanar angle 2.5°), eclipsed, and rotated by only 3.9° against each other. Thus, the two substituents lie one above the other; however, they are not coplanar with the respective Cp plane, but rotated by 36 and 30°, and the two benzodithiol fragments R and R' are not parallel,

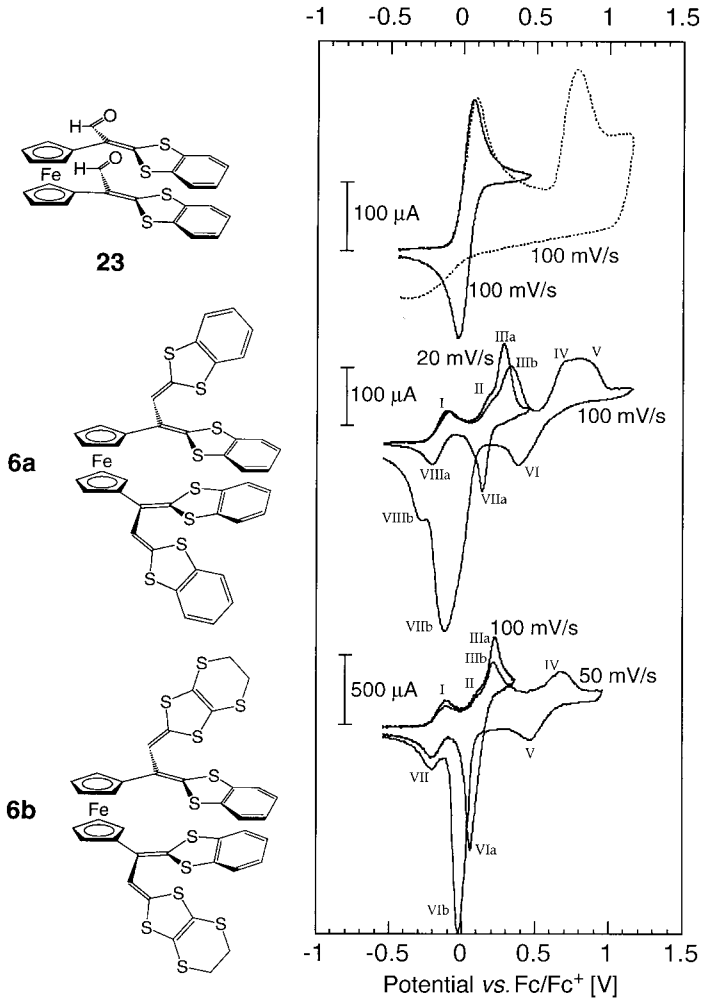

Fig. 3. *Cyclovoltammograms of the two ferrocene-bridged vinylogous TTF derivatives* **6a** *and* **6b** *and of their precursor* **23**

with an interplanar angle 14.4°. The distances between the planes of the two neighboring benzene rings are between 3.88 and 4.52 Å, which is larger than a *van der Waals* stacking distance. The two aldehyde groups lie in the same plane as the benzodithiol fragments, as indicated by the distances of the O-atoms from the corresponding planes of 0.3 Å for O(1) and 0.02 Å for O(1′). There are quite short contacts between the S- and O-atoms of 2.66 and 2.61 Å, respectively. Also, the bond distances C(6)–C(14) and C(6′)–(14′) are shorter than expected (1.440(4) and 1.436(5) Å, resp.). Both anomalies may indicate a contribution of a thienium/enolate resonance structure, thus with an attractive S–O interaction.

Crystals of the ferrocene-bridged vinylogous TTF derivative **6a** are triclinic (space group $P\bar{1}$) with two different molecules per asymmetric unit. These two molecules,

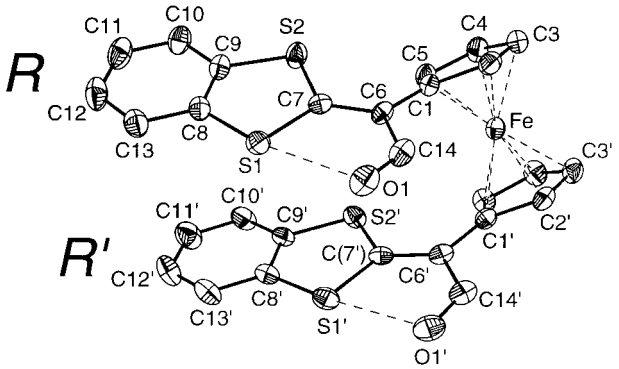

Fig. 4. *ORTEP Plot of dialdehyde* **23** *with the atom-numbering scheme.* Thermal ellipsoids are drawn at the 30% probability level; H-atoms are omitted.

indicated hereafter as M_A and M_B, with the benzodithiol fragments *R1* and *R1′* (closer to the Cp ring), and *R2* and *R2′* (further away from the Cp ring), respectively, are enantiomers (*Fig. 5*). The molecules are pseudo-C_2-symmetric with eclipsed and parallel Cp rings that are rotated against each other by 79 (M_A) and 68° (M_B). The benzene rings in the fragments *R1* and *R1′* stack in a 'face-to-face' geometry with distances of 3.64 (M_A) and 3.89 Å (M_B), slightly larger than *van der Waals* contacts. The corresponding interplanar angles are 2.7 (M_A) and 2.9° (M_B). On the other hand, the fragments *R2* and *R2′* are almost perpendicular to the fragments *R1* and *R1′*, with torsion angles C(7)–C(6)–C(14)–C(15) of 83 and 79° (M_A), and −94° and −86° (M_B), thus indicating that there is no conjugation between *R1* and *R2*.

The very similar ferrocene-bridged TTF derivative **6b** also crystallizes in the triclinic space group $P\bar{1}$. However, crystals contain two CH_2Cl_2 molecules per asymmetric unit, one of which is highly disordered (see *Fig. 6*). Again, the two Cp rings are eclipsed (interplanar angle 5.8°) and rotated against each other by 86°. The two fragments *R1*/*R1′* and *R2*/*R2′* are again not coplanar. The torsion angle C(8)–C(6)–C(7)–(15) is −68° (and −141° for the corresponding angle of *R1′* and *R2′*). With respect to **6a**, the most striking difference is that the two benzene rings of the fragments *R1* and *R1′* in **6b** show an 'edge-to-face' interaction with an interplanar angle of 60° and a distance of the two ring centers of 5.1 Å.

The vinylogous ferrocenyl-substituted TTF derivatives **21c** and **21d** are isomorphous and crystallize in the non-centrosymmetric space group $P2_12_12_1$. A view of the asymmetric unit of **21c** and **21d**, along with the atom-numbering scheme, is depicted in *Fig. 7*. Like the compounds **6a** and **6b**, the vinylogous TTF substituents are not planar, and the fragment *R1* is not coplanar to the respective Cp ring. The interplanar angle between *R1* and *R2* is 58° for **21c** and 56° for **21d**. The torsion angle C(7)–C(6)–C(12)–C(13) is 64° (−67°), and the plane of *R1* forms an angle with the Cp ring of 42° (48°).

2.3.3. *Charge-Transfer Complexes.* The apparently small difference between [*meso*-Fe{η^5-C_5Me_3(S^{t}Bu)}$_2$][Ni(mnt)$_2$] (**26**) and the corresponding octamethylated derivative [1] has a remarkably strong influence on the relative arrangement of the molecules in the solid state. Thus, whereas the latter displays a typical $D^+A^-D^+A^-$ structure, in **26**

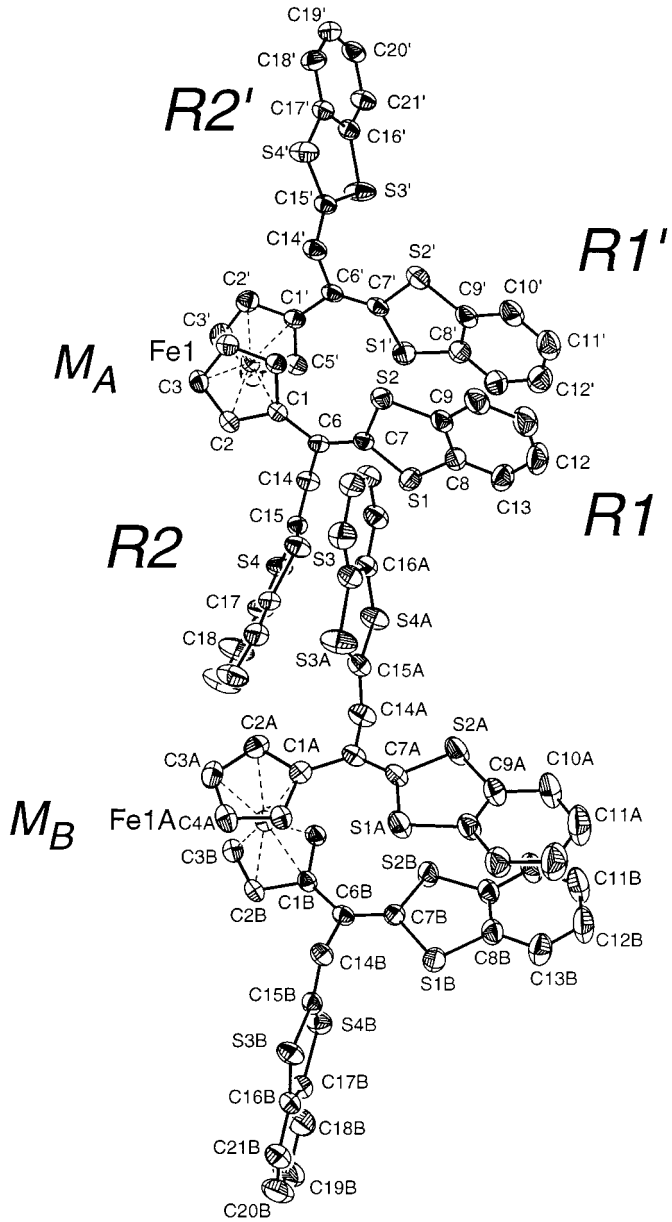

Fig. 5. *ORTEP Plot of the asymmetric unit with the two enantiomers* M_A *and* M_B *in* **6a**, *with the atom-numbering scheme.* Thermal ellipsoids are drawn at the 30% probability level; H-atoms are omitted.

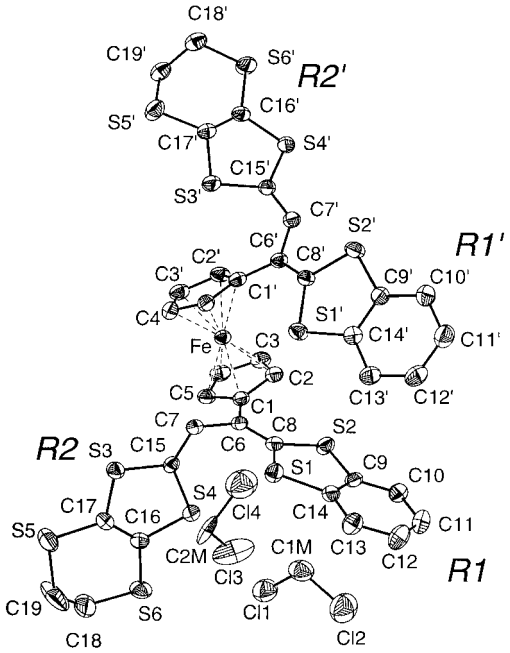

Fig. 6. *ORTEP Plot of the asymmetric unit of the ferrocene bridged vinylogous TTF derivative* **6b**, *with the atom-numbering scheme.* Thermal ellipsoids are drawn at the 30% probability level; for clarity reasons, the second position of the C-atom C2M in the disordered solvent molecule (occupancy 25%), as well as H-atoms, are omitted.

there are layers of ferrocenium cations alternating with layers of $[(Ni(mnt)_2)_2]^{2-}$ anion pairs, running diagonally through the unit cell. A projection along the *b* axis of a pair of such layers is depicted in *Fig. 8*, and a projection along the *a* axis is given in *Fig. 9*. It is apparent that the anion dimers are well separated from each other. Within each dimer, the two anions are arranged in such a way that each Ni-atom lies above the C=C bond of the neighboring unit (see also below, *Fig. 17*). A consequence of this arrangement is that two pairs of S-atoms lie above each other with intermolecular S–S distances of 3.72 Å, and that the Ni–Ni distance becomes quite large (4.54 Å). Another feature of this structure is that the $[Ni(mnt)_2]^-$ units quite strongly deviate from planarity, as indicated by the interplanar angle between the two mnt ligands of 10.4°. To the best of our knowledge, this type of structure in $[Ni(mnt)_2]^-$ dimers has never been observed before and, as we will see, has an important effect on the magnetic properties of the CT complex **26**. Finally, the cations show a pseudo-centrosymmetric conformation, with parallel Cp rings (interplanar angle $< 0.5°$) rotated against each other by 178°.

The platinum derivative **27** crystallizes in the orthorhombic space group *Pbca*, with both the Fe- and the Pt-atoms on symmetry centers. Thus, every cation is completely surrounded by six anions, resulting in a three-dimensional $D^-A^+D^-A^+$ motif. A projection of a layer perpendicular to the *c* axis is depicted in *Fig. 10*. Within such a layer, four $[Pt(mnt)_2]^-$ anions assume a propeller-like arrangement around the cation (symmetry center), with an interplanar angle of 74° within each pair. One of the nitrile

groups points almost directly to the Pt-atom of the neighboring anion, with a Pt–N distance of 5.77 Å. The same N-atom has an equal distance to the Fe-center. The three different Fe–Pt distances are 6.65 Å along *a*, 8.42 Å along *b*, and 8.65 Å along *c*, corresponding to half-cell constants. The Cp ring of the cation is almost parallel to the anions in the *a* direction (interplanar angle 7.2°).

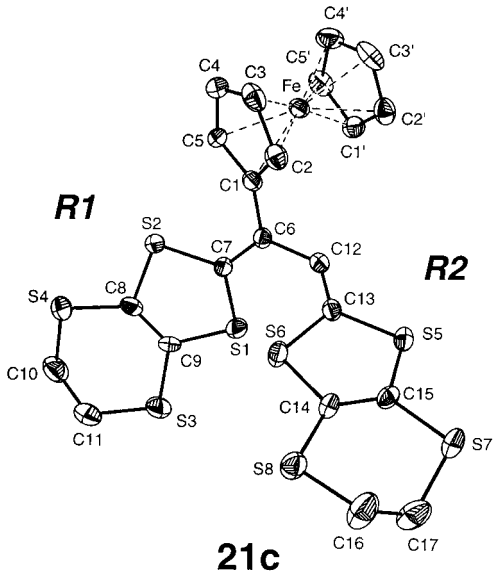

21c

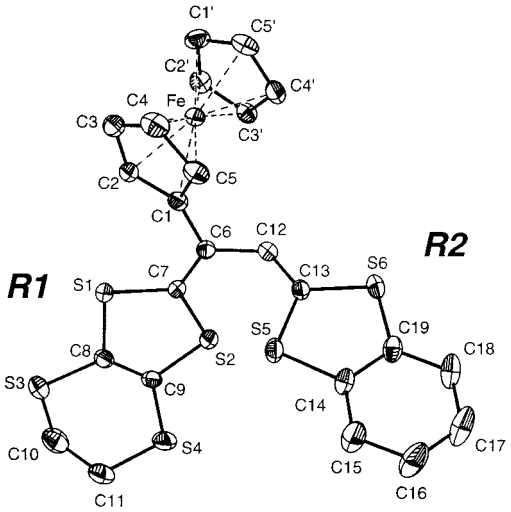

21d

Fig. 7. *ORTEP Plot of the asymmetric unit of the vinylogous TTF derivatives* **21c** *and* **21d** *with the atom-numbering scheme.* Thermal ellipsoids are drawn at the 30% probability level; H-atoms are omitted.

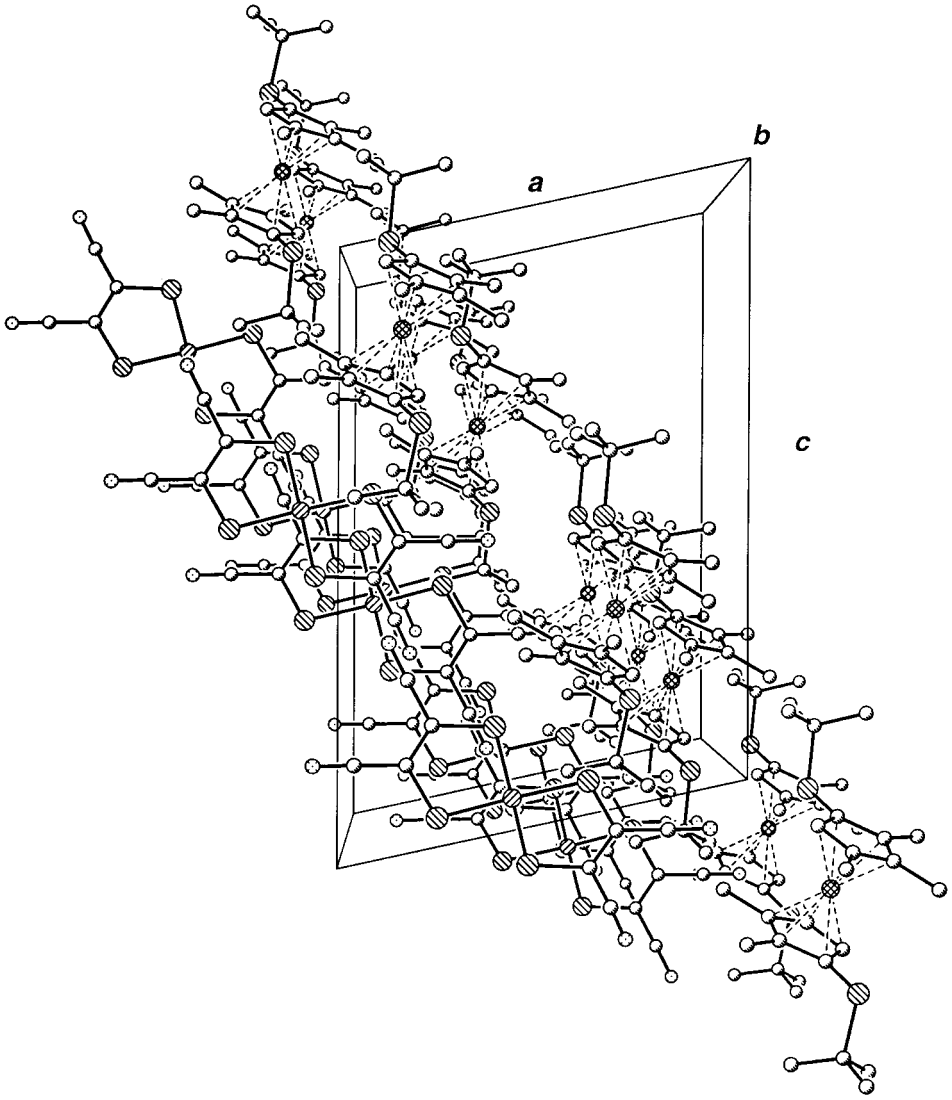

Fig. 8. *Perspective view of a ferrocenium and [Ni(mnt)$_2$]-layer of* **26** *projected along the* b *axis*

The CT complex **28** of the 1,1′,2,2′,3,3′,4,4′-octamethyl-5,5′-trithioferrocene (**4**) and $[Ni(mnt)_2]^-$ crystallizes in the monoclinic space group $P2_1/c$ and displays a $D^+D^+A^-A^-D^+D^+A^-A^-$ motif. The structure consists of alternating planes of almost perpendicular stacks. A projection along one of the stacking directions is depicted in *Fig. 11*, and a side view of a stack is detailed in *Fig. 12*. Two anions from two neighboring layers form an interplanar angle of 74°. The $[Ni(mnt)_2]^-$ dimers have structural features as previously found in other compounds [1][28][29], with each Ni-atom interacting with a S-atom of the companion fragment at a distance of 3.78 Å.

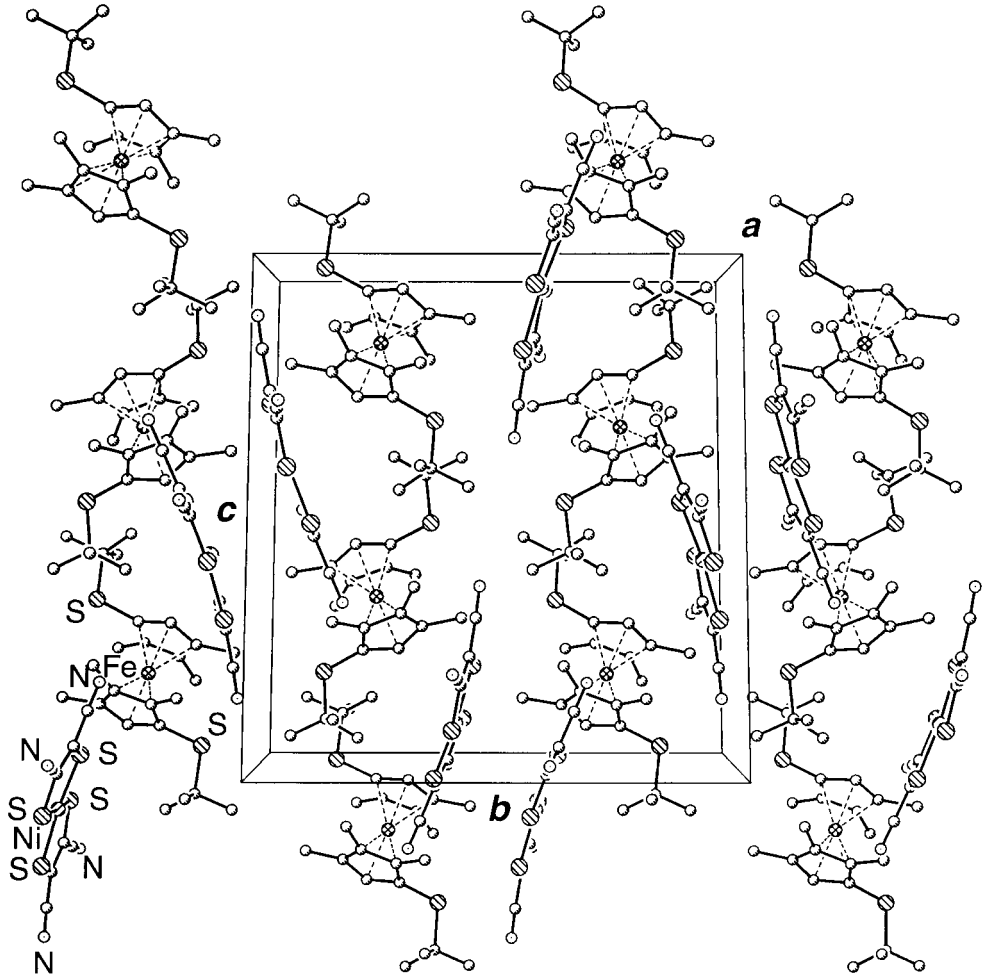

Fig. 9. *Perspective view of a ferrocenium and [Ni(mnt)$_2$]-layer of* **26** *projected along the* a *axis*

Furthermore, the Ni-atoms show a weak interaction with the terminal S-atom of the trithio unit at a distance of 3.86 Å. The Cp ring of the cation is almost perfectly parallel to the anion plane, with an interplanar angle of less than 2°. The cations within a pair are facing each other with an intermolecular distance between the middle disordered S-atoms of 3.53 Å, similar to what was found for the corresponding $[FeCl_4]^-$ and $(TCNQF_4)^-$ salts [5][7] ($(TCNQF_4)^- =$ '2,3,5,6-tetrafluorotetracyanoquinodimethanide').

A comparable description may be applied to the structure of the triclinic **30**, crystallizes in the space group $P\bar{1}$. Again a $D^+D^+A^-A^-D^+D^+A^-A^-$ motif is observed, however, with the anions being almost congruent one above the other, with Ni–Ni (3.64 Å) and S–S (3.56 Å and 3.65 Å) interactions, as shown in *Fig. 13*. As opposed to the octamethylated derivatives previously reported by *Hobi et al.* [4][6], the S-heterocycle in the cation resulting from **5** is almost coplanar to the Cp ring, with an

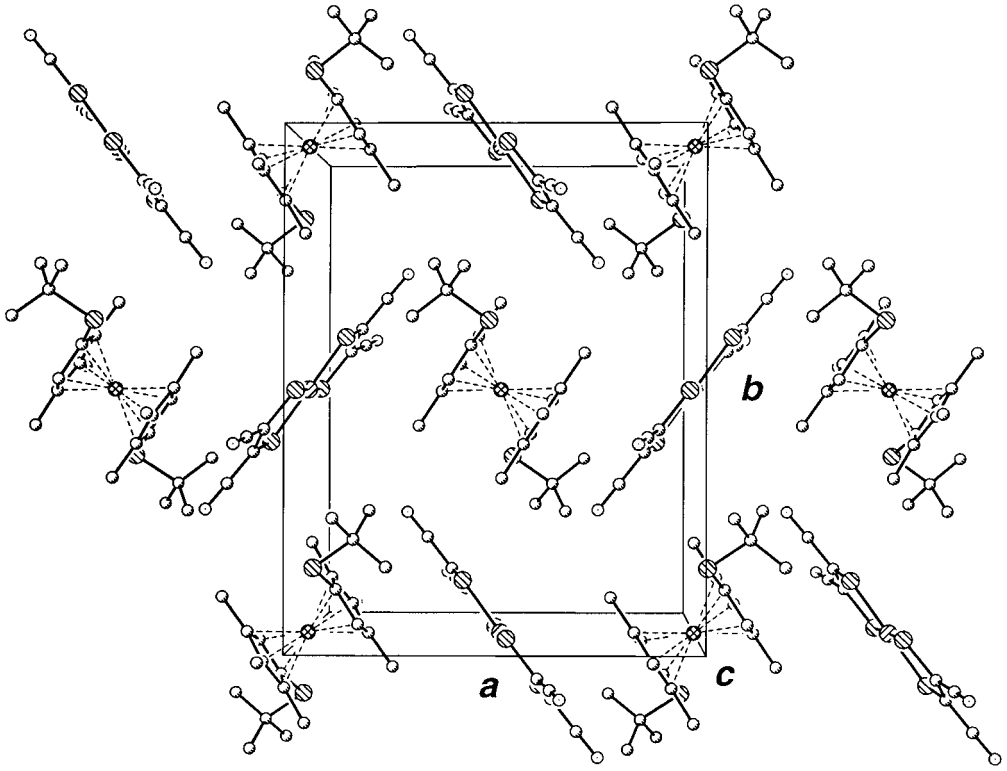

Fig. 10. *Perspective view of a layer of cations and anions perpendicular to the* c *axis in* **27**

interplanar angle between the Cp ring and the heterocycle of 11°. A cation/anion interaction exists, as represented by a Ni–S contact distance of 3.80 Å of one of the two S-atoms. The other one has short-range interactions (3.66 and 3.59 Å) with two S-atoms of a $[Ni(mnt)_2]^-$ dimer in the neighboring layer. Two neighboring donor molecules constitute an enantiomeric pair, with a symmetry center located between the two parallel benzene rings. The planes of the latter are separated from each other by *ca.* 3.66 Å, slightly larger than typical *van der Waals* contacts. Finally, there is one dichloroethane molecule per donor/acceptor unit with a Cl–C–C–Cl torsion angle of 63°. Th solvent molecules form a zig-zag arrangement parallel to the *b* axis, with alternating short (3.35 Å) and long (3.45 Å) Cl–Cl-distances.

Compound **31a** crystallizes in the monoclinic space group *C*2/*c* with segregated stacks of donor and acceptor molecules. The acceptor stacks contain intercalated dichloroethane molecules, thus leading to a large Ni–Ni distance of 8.31 Å. The ferrocene molecules adopt a chiral conformation and lie on the twofold axes parallel to the *b* axis. All molecules aligned on one such C_2 axis show the same orientation and absolute configuration. Thus, enantiomerically pure stacks of each enantiomer alternate along the *c* axis, as evident from both the projection of the unit cell along the *a* axis in *Fig. 14* and a projection along the C_2 axis in *Fig. 15*. The overall conformation of the ferrocenium cations is very different from that of the neutral

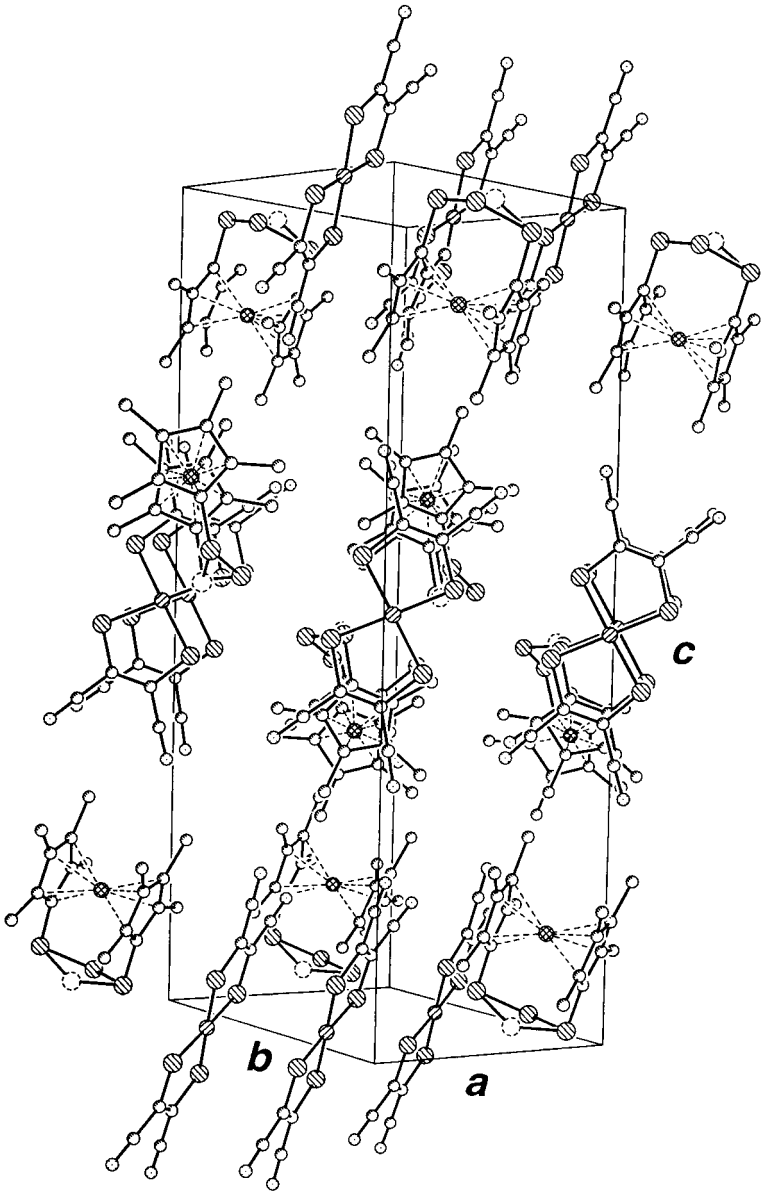

Fig. 11. *Perspective view of the unit cell of* **28**, *projected along one stacking direction*

molecule **6a**. The two Cp rings show an eclipsed conformation with the two substituents directly above each other, and a relatively large opening of 13° in the direction of the substituents. Thus, the distances C(3)–C(4′) and C(4)–C(3′) are shortened to 3.17 Å and C(1)–C(1′) is elongated to 3.69 Å from the value of 3.37 Å in ferrocene. The orientation of the two heterocyclic fragments *R1* is such that only the five-membered

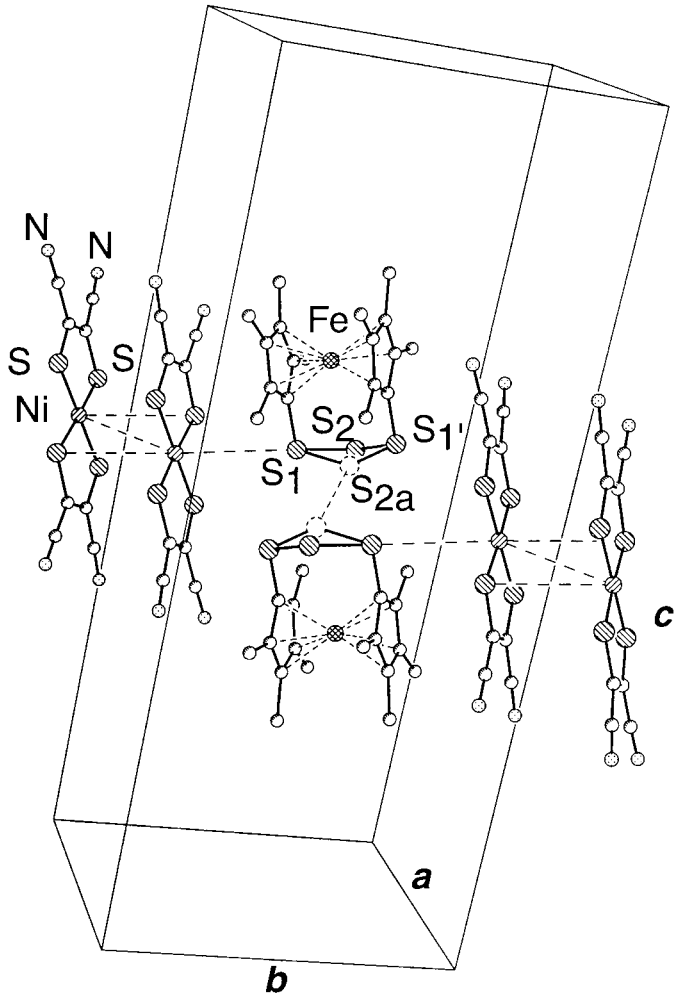

Fig. 12. *Side view of a* $A^-A^-D^+D^+A^-A^-$ *stack in* **28**

rings overlap to a significant extent, with relatively short distances of 3.75 Å between S(2) and S(2′). The two fragments *R1* and *R2* are now more planar than in the neutral molecule. The torsion angle around the bond C(6)–C(14) within the vinylogous TTF unit is 147° (83°, 94° in neutral **6a**). Thus, this unit approaches coplanarity of the two heterocycles (interplanar angle of 34°) much more than does the neutral molecule, where the two fragments are almost perpendicular to each other. A significant conjugation and hence delocalization of positive charge is therefore possible, despite the rotation by 47° of the substituents with respect to the Cp ring. Donor-donor intermolecular interactions are also apparent. Along the *a* axis, *e.g.*, the atoms S(1) in fragments *R1* are separated by 3.57 Å, which is significantly shorter than *van der Waals* distance (3.7–4.1 Å). Moreover, along the *c* axis, the fragments *R2* show a plane-to-plane distance of 3.5 Å, which corresponds to the *van der Waals* distance of the S- and

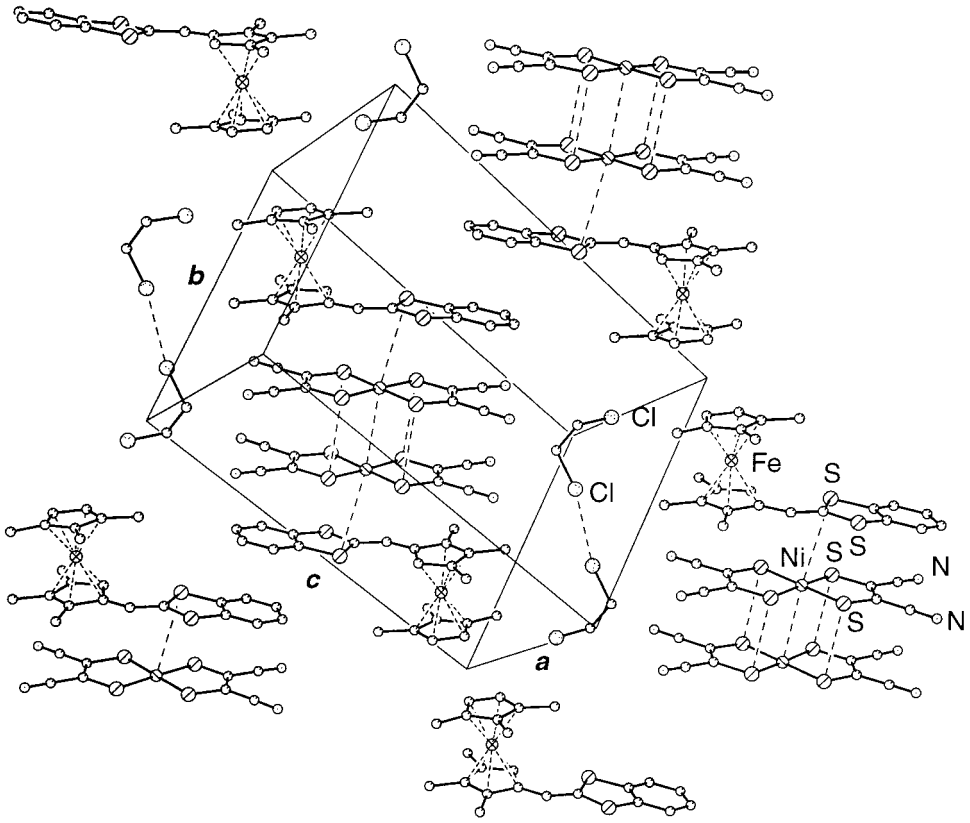

Fig. 13. *Perspective view of a layer of* **30**, *projected perpendicular to the layer plane.* Contacts which are shorter than *van der Waals* distances are indicated by dotted lines. The dichloroethane molecules fill the empty space between two $D^+A^-A^-D^+$ packages.

C-atoms. This leads to a two-dimensional network of stacking interactions between donor molecules (*Fig. 14*). The perfectly planar anions, which lie on a symmetry center, fill the space between the layers of the ferrocenes and are, therefore, strongly separated. The shortest contact of a S-atom of the anion and *R2*, *e.g.*, is more than 4 Å.

2.4. *Magnetic Measurements.* Magnetic-susceptibility measurements were carried out for the CT complexes **26**–**31a** with a SQUID (superconducting quantum interference device) susceptometer in the temperature range between 2 and 300 K at a constant external field of 1000 Gauss. All compounds except **31a** obey a modified *Curie-Weiss* expression (*Eqn. 1*), where q is the sum of core diamagnetism and temperature-independent paramagnetism (TIP)[1]). For all compounds, q is positive, meaning that TIP is larger than the diamagnetic component.

$$\chi_{mol} = \frac{C}{T-\theta} + q \qquad (1)$$

[1]) q = sum of χ_{DIA} and χ_{TIP}; $\langle g_A \rangle = 2.01$ [37].

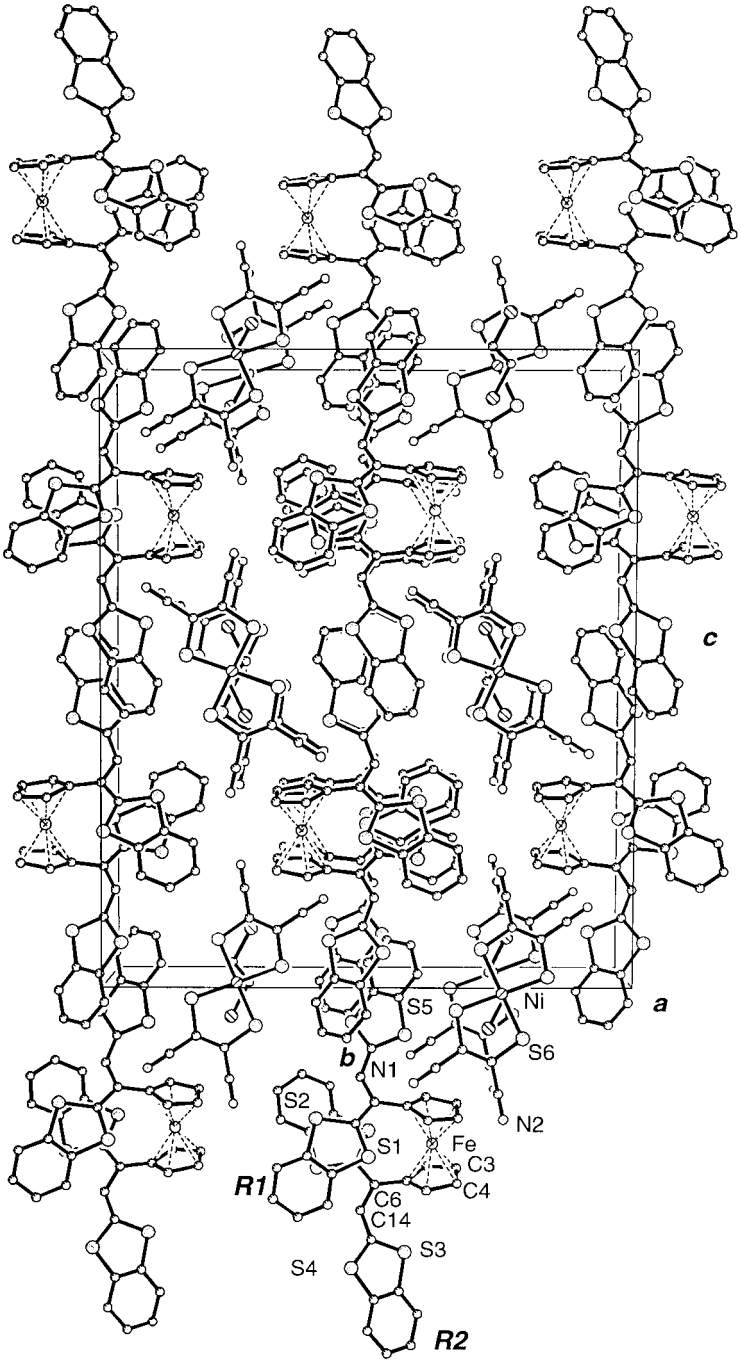

Fig. 14. *Perspective view of the unit cell of* **31a**, *projected along the* a *axis.* Numbering of the atoms and fragments as described in the text.

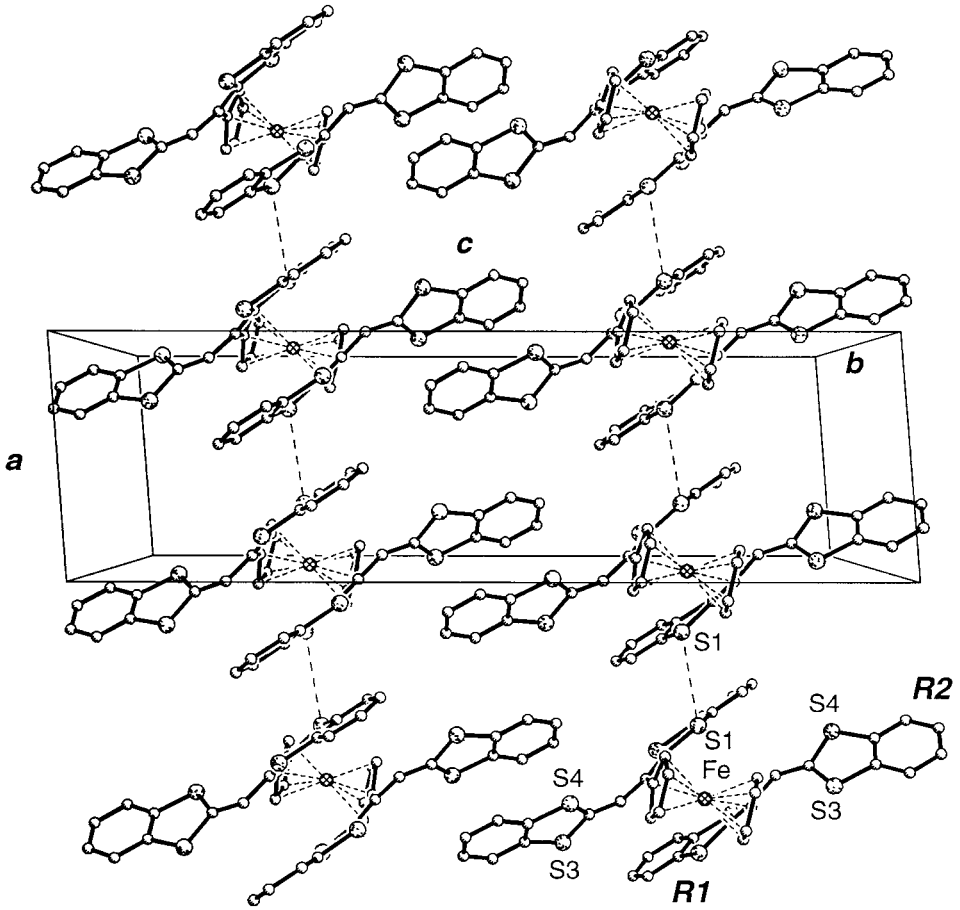

Fig. 15. *Perspective view of a ferrocenium layer of* **31a**, *projected along the* b *axis.* There are short contacts between the S-atoms S(1) (3.57 Å, dotted lines) of the fragments *R1*.

A plot of $\chi_{mol}T$ *vs.* T for the six compounds is shown in *Fig. 16*. The magnetic properties of the CT complexes are strongly influenced by the relative arrangement of the molecular components in the crystal. In principle, there are two main structural classes, *i.e.*, one with separated single anions and cations assuming a $D^+A^-D^+A^-$ arrangement, and showing ferromagnetic interactions (*e.g.* **27**) [1][30], and a second group containing dimers of anions, this being the more common case. This second group can in turn be divided in two subgroups: those with isolated dimers displaying a $D^+A^-A^-D^+$ motif (for example **28** and **30**), and those with segregated stacks of anion dimers and columns of cations. For this second category, many examples have been reported [1][3][28][30–32]. *Weiher* and co-workers [31] found in 1964 that the tetraethylammonium salts of $[\{M(mnt)_2\}_2]^{2-}$ (M = Ni, Pt) have a singlet ground state ($S = 0$) with a thermally populated excited triplet state ($S = 1$). These authors used the

equation developed by *Figgis* and *Martin* [33] (*Eqn. 2*)[2]) to calculate the molar magnetic susceptibility of dimeric $[\{M(mnt)_2\}_2]^{2-}$ complexes, and found an energy gap between singlet and triplet state J_{AA} ($S=0 \rightarrow S=1$) for $(Et_4N)[Ni(mnt)_2]$ of 620 cm^{-1}.

$$\chi_{mol} = \frac{N\beta^2\langle g_A\rangle^2 S_A(S_A+1)}{kT(3+e^{-J_{AA}/kT})} + \chi_{DIA} + \chi_{TIP} \quad (2)$$

Twenty years later, *Ramakrishna* [34] showed that this is not a sufficiently accurate description because, in a stack of anions with alternating distances, alternating J values should be observed. It has been shown that these values are extremely sensitive to the packing arrangement of the dimers. Unfortunately, it is not easy to discern the two different values from only temperature-dependent susceptibility measurements, because there are too many parameters to fit. However, *Eqn. 2* can be used as long as the observed J values are interpreted as average values for all possible interactions. A survey of the magnetic data of the new compounds, together with some selected literature data, are given in *Table 3*.

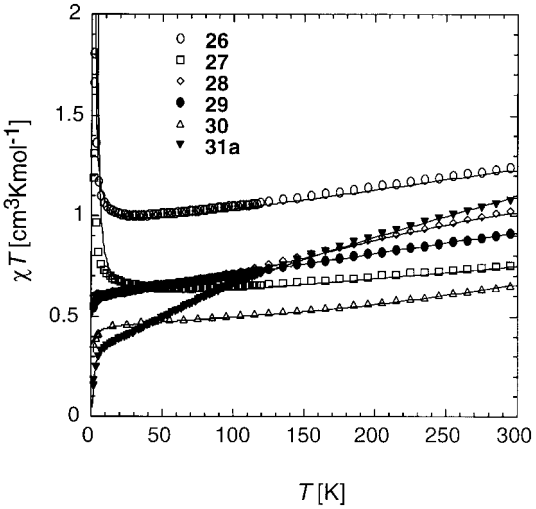

Fig. 16. *SQUID Susceptibility data for compounds* **26**–**30** *and* **31a** *measured in an external field of 1000 G.* The lines correspond to the calculated values either with *Eqn. 1* (**26**, **27**) or *Eqn. 4* (**28**–**30**, **31a**).

With the assumption that there are no interactions between the ferrocenium donors and the $[\{Ni(mnt)_2\}_2]^{2-}$ dimers, the magnetic susceptibility of both components is additive (*Eqn. 3*) [35]. This assumption is meaningful whenever the metal-metal distances between donors and acceptors are sufficiently large. For both contributions, χ_{donor} and $\chi_{acceptor}$, a term as in *Eqn. 2* can be used to calculate the molar magnetic susceptibility of the compounds containing $[\{M(mnt)_2\}_2]^{2-}$ dimers, as given by *Eqn. 4*.

---

[2]) *N*, *Avogadro* constant; β, *Bohr* magneton; $\langle g_A\rangle$, average *Landé* factor of the acceptors; S_A, spin of the acceptors; k, *Boltzmann* constant; J_{AA}, energy difference between ground and excited state; χ_{DIA}, diamagnetic susceptibility; χ_{TIP}, temperature-independent paramagnetic susceptibility.

Table 3. *Survey of the Observed Magnetic Data for the Charge-Transfer Complexes* **26**–**30** and **31a**, *as well as for Some Selected Previously Reported Compounds*

	Curie constant C [cm^3Kmol^{-1}]	μ_{eff} [$\mu_b mol^{-1}$]	*Weiss* Const. θ [K]	J_{AA} [cm^{-1}]	J_{DD} [cm^{-1}]	$\langle g_D \rangle$	$q \cdot 10^{-6}$ [cm^3mol^{-1}]
26	0.917(5)	2.71	+1.3(2)	–	–	2.40	1031(17)
27	0.554(4)	2.10	+3.0(49)	–	–	1.37	631(18)
28	0.559(5)	2.11	+0.7(3)	−302(8)	−0.27(5)	2.588(5)	607(25)
29	0.6048(4)	2.20	−0.197(4)	< −1000	−0.459(9)	2.9035(9)	1047(3)
30	0.402(6)	1.79	+1.3(6)	−630(33)	−1.01(7)	2.192(8)	477(36)
31a	0.451(5)	1.90	−6.0(59)	−96(1)	−2.34(3)	2.280(3)	1889(4)
$(Et_4N)[Ni(mnt)_2]$ [29][31]	–		–	−620	–	2.06[37]	−260
$(Ph_3MeP)[Ni(mnt)_2]$ [28][31]	–		–	−490	–	2.06[37]	−150
$(Et_4N)[Pt(mnt)_2]$ [31][32]	–		–	−350	–	2.04[37]	−220
[**1**][$Ni(mnt)_2$] [1][7]	0.88(2)	2.65	−0.7(9)	−6(1)	+0.6(4)	2.65(4)	720(50)
$[Fe(\eta^5\text{-}C_5H_4CHCHPhSMe)_2]$-$[Ni(mnt)_2]$ [3][6]	0.480(4)	1.96	+0.7(4)	−771(4)	−0.81(3)	2.692(4)	626(15)

$$\chi_{mol} = \chi_{donor} + \chi_{acceptor} + \chi_{DIA} + \chi_{TIP} \tag{3}$$

$$\chi_{mol} = \frac{N\beta^2}{kT}\frac{\langle g_D \rangle^2 S_D(S_D+1)}{3+e^{-J_{DD}/KT}} + \frac{\langle g_A \rangle^2 S_A(S_A+1)}{3+e^{-J_{AA}/KT}} \tag{4}$$

We shall address the CT complexes **28** and **30** first, as they contain isolated $[Ni(mnt)_2]^-$ dimers displaying a known arrangement within the $D^+A^-A^-D^+$ motif. Furthermore, although the crystal structure of **29** is not known, the magnetic data strongly indicate that its structure must be very similar to that of **28**. Thus, for these compounds, the *Curie* constants C are too small for one unpaired electron per donor and acceptor molecule ($C = 0.559(5)$ cm^3K/mol and $\mu_{eff} = 2.11\ \mu_B mol^{-1}$ for **28**[3]); $C = 0.6048(4)$ cm^3K/mol $\mu_{eff} = 2.20\ \mu_B mol^{-1}$ for **29**; $C = 0.402(6)$ cm^3K/mol and $\mu_{eff} = 1.79\ \mu_B mol^{-1}$ for **30**). By fitting the observed data with *Eqn. 4*, strong antiferromagnetic interactions for all three compounds result, as expected (**28**: $J_{AA} = -302(8)\ cm^{-1}$ and $J_{DD} = -0.27(5)\ cm^{-1}$; **29**: $J_{AA} < -1000\ cm^{-1}$ and $J_{DD} = -0.459(9)\ cm^{-1}$; **30**: $J_{AA} = 630(33)\ cm^{-1}$ and $J_{DD} = -1.01(7)\ cm^{-1}$). The higher value of J_{AA} for **30**, as compared to **28**, can be explained by the relatively strong direct Ni–Ni interaction, whereas in **28**, a Ni–S–Ni interaction is found. In the Pt derivative **29**, the coupling constant J_{AA} is too large for it to be obtained by means of magnetic-susceptibility measurements. In other words, in the measured temperature range below 300 K, only the contribution of the cation is observed. Because of the relatively short distances of one S-atom of the donors to the Ni-atom of the acceptors in **28** and **30**, a D^+A^- interaction could be expected. However, below 100 K, the triplet state of the $[\{Ni(mnt)_2\}]^-$ dimers is no longer thermally populated, such that the contribution of an interaction between donor and acceptor has no significant influence on the magnetic susceptibility below this temperature.

The magnetic behavior of **31a** is more complex, as it does not obey the *Curie-Weiss* expression (*Eqn. 1*). Nevertheless, a *Curie* constant C of 0.451(5) cm^3K/mol ($\mu_{eff} = 1.90\ \mu_B mol^{-1}$) and a negative *Weiss* constant θ of −6.0(5) K could be determined. The

[3]) As obtained from high-temperature data according to $\mu_{eff} = (3k\chi_{mol} \cdot T/N\beta^2)^{1/2}$), calculated per 1 mol of Fe.

χT *vs.* T plot (*Fig. 16*) shows a steady decrease with a small plateau at about 25 K and a strong drop below 10 K. This behavior points out strong antiferromagnetic interactions. Although it is possible to obtain perfect coincidence between values calculated with *Eqn. 4* and the observed measured data, the resulting values for J_{AA} and J_{DD} probably do not have any physical meaning. It is indeed known from the crystal structure (*vide supra*) that there are several contacts between the donor molecules and also between donors and acceptors, possibly leading to magnetic couplings.

As opposed to the above compounds, **26** shows a strong increase in χT as a function of T below 20 K (*Fig. 16*). The *Curie* constant C of 0.917(5) cm^3K/mol ($\mu_{eff} = 2.71\,\mu_B mol^{-1}$) indicates that there has to be an unpaired electron per donor and acceptor molecule ($S = 2 \times 1/2$ spin system). Thus, the hitherto unknown arrangement of the $[Ni(mnt)_2]^-$ anions within a dimer changes the sign of the spin-spin interaction. This is the first time that an isolated $[\{Ni(mnt)_2\}_2]^{2-}$ dimer with a ferromagnetic ($S = 1$) ground state has been found. A comparable situation was reported for the $[Ni(dmit)_2]^-$ salt of decamethylferrocenium [36]. This observation can now help to explain the unusually weak antiferromagnetic interaction in the previously described compound [**1**] $[Ni(mnt)_2]$ [1]. In this compound, stacks of $[\{Ni(mnt)_2\}_2]^{2-}$ dimers are found, like in $(Et_4N)[Ni(mnt)_2]$. However, the interdimer interaction is probably a ferromagnetic one as in **26**, of almost the same magnitude as the antiferromagnetic intradimer interaction. Such an alternation of ferromagnetic and antiferromagnetic interactions leads to the overall weak antiferromagnetic J_{AA} value of only $-6(1)\ cm^{-1}$. A summary of the observed magnetic properties of $[Ni(mnt)_2]^-$ dimers in different CT complexes, along with a view of the different dimer arrangements, is depicted in *Fig. 17*.

Compound **27** shows behavior similar to that of its companion **26**, with the difference that the *Curie* constant C is too small for it to indicate the presence of one unpaired electron per molecular unit ($C = 0.554(4)\ cm^3K/mol$, $\mu_{eff} = 2.10\,\mu_B mol^{-1}$). This can be explained only with an exceptionally small average *Landé* factor $\langle g_D \rangle$ for the ferrocenium cation of only 1.37 ($\langle g_A \rangle$ for $[Pt(mnt)_2]^- = 2.04$ [37]). Below 20 K, again a strong increase is observed in the χT *vs.* T plot (*Fig. 16*), indicating a weak but significant ferromagnetic ordering at low temperature, as shown also by the positive *Weiss* constant θ of $+3.04(4)$ K. This observation is in accord with the $D^+A^-D^+A^-$ arrangement of the molecules found in the solid state.

3. Conclusions.– We have shown that it is possible to achieve ferromagnetic interactions in molecular materials containing $[M(mnt)_2]^-$ anions by two completely different interaction pathways. One of them is the already known mechanism relying upon a $D^+A^-D^+A^-$ structural motif, as in compound **27**. The second one is based on the new dimer arrangement found in [*meso*-Fe{η^5-$C_5HMe_3(S^tBu)$}$_2$][$Ni(mnt)_2$] (**26**), leading to a dimer with a ferromagnetic ground state. Therefore, it should be possible, in principle, to obtain a one dimensional stack of ferromagnetically coupled $[M(mnt)_2]^-$ anions, as long as the cation would favor such a relative arrangement of the anions. However, we have seen how serendipitous and unpredictable the structural properties of $[M(mnt)_2]^-$ CT complexes are, also in view of the structural variety of the ferrocenyl donor molecules. Thus, the goal remains to find ferromagnetic compounds with higher T_c's than for the $D^+A^-D^+A^-$ complexes of decamethyl ferrocene with TCNE (tetracyanoethylene = ethenetetracarbonitrile) and TCNQ (= tetracyano-

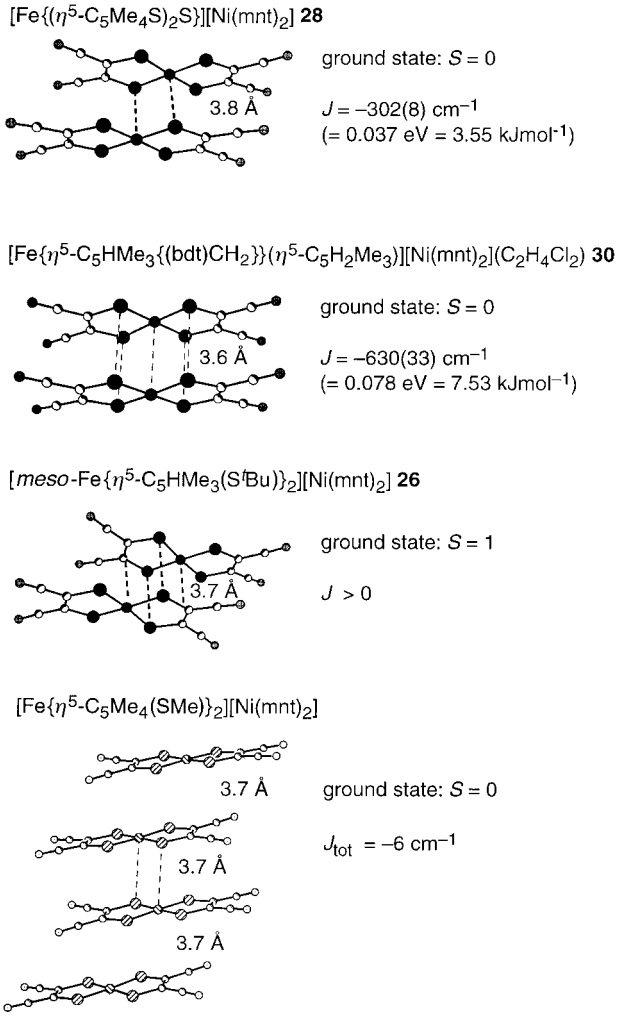

Fig. 17. *Different arrangements of [[Ni(mnt)$_2$]$_2$]$^{2-}$ dimers, with their magnetic interaction parameters* J. In the ferromagnetically coupled compound **26**, the value of *J* could not be determined, because of an over-parameterization.

quinodimethane = 2,2′-(cyclohexa-2,5-diene-1,4-diylidene) bis[propanedinitrile]) reported by *Miller* and others [38–41]. We are currently performing quantum-mechanical calculations aimed at finding the relative energy differences in the three different dimer arrangements, and to calculate the triplet/singlet energy gap in **26**.

Experimental Part

General. Experimental techniques were described earlier [2]. NMR: at 250.13 (^{1}H) and 62.895 MHz (^{13}C) for $CDCl_3$ solns. at 25°, unless stated otherwise; δ in ppm rel. to $SiMe_4$ (= 0 ppm), *J* in Hz. MS: *m*/*z* (rel. %).

*1-[(*tert*-Butyl)thio]-2,3,4-trimethylcyclopenta-1,3-diene* (**8**). A soln. of 2,3,4-trimethylcyclopent-2-en-1-one [8][9][42–46] (**7**; 4.958 g, 39.9 mmol) in THF (100 ml) was mixed with titanium tetrachloride (6.77 g,

35.7 mmol) at 0°, and sodium 1,1-dimethylethanethiolate (4.475 g, 39.9 mmol) and Et_3N (5.56 mL, 39.9 mmol) were added dropwise. The mixture was warmed to r.t. and stirred overnight. The solvent was evaporated and the residue distilled at 110°/$3 \cdot 10^{-2}$ mbar in a bulb-to-bulb distillation apparatus: 4.56 g (58%) of **8**. Bad smelling yellow oil. ^{1}H-NMR: 1.28 (*s*, *t*-Bu); 1.83 (*s*, 1 Me); 1.94 (*s*, 1 Me); 2.01 (*s*, 1 Me); 3.02 (*m*, CH_2). ^{13}C-NMR: 11.30 (Me); 13.39 (Me); 13.56 (Me); 31.44 (*Me*$_3$C); 46.95 (Me$_3$*C*); 52.16 (CH_2); 124.83 (Me*C*); 136.40 (Me*C*); 138.85 (Me*C*); 142.65 (^{t}BuS*C*). EI-MS: 196.3 (42; $M^{+\bullet}$), 140 (100), 125, 107.

*1,1′-Bis[(*tert*-butyl)thio]-2,2′,3,3′,4,4′-hexamethylferrocene* (mixture of diastereoisomers **3a**/**3b**). The same procedure as for 1,1′-bis[(*tert*-butyl)thio]-2,2′,3,3′,4,4′,5,5′-octamethylferrocene [1] was applied, with **8** (4.15 g, 21.1 mmol), THF (30 ml), a freshly prepared lithium diisopropylamide (LDA) soln. (from (^{i}Pr)$_2$NH (4.5 ml), 1.6M BuLi in hexane (17 ml), and THF (25 ml)), and anh. iron(II) chloride (2.08 g, 29.6 mmol): 2.89 g (70%) of **3a**/**3b** 1:1. M.p. 101°. By recrystallization from hexane, the *meso*-form **3a** could be enriched to a *meso*/*rac* ratio of 85:15 after one recrystallization.

Data of **3a**: ^{1}H-NMR: 1.15 (*s*, 2 *t*-Bu); 1.79 (Me); 1.84 (Me); 1.86 (Me); 3.67 (*s*, 2 CH (Cp)). ^{13}C-NMR: 10.32 (Me); 10.99 (Me); 11.75 (Me); 30.84 (*Me*$_3$C); 44.89 (Me$_3$*C*); 74.94 (CH (Cp)); 78.07 (^{t}BuS*C*); 83.11 (Me*C* (Cp)); 83.48 (Me*C* (Cp)); 86.05 (Me*C* (Cp)).

Data of **3b**: ^{1}H-NMR: 1.15 (*s*, 2 *t*-Bu); 1.80 (*s*, 2 Me); 1.81 (*s*, 2 Me); 1.85 (*s*, 2 Me); 3.78 (*s*, 2 CH (Cp)). ^{13}C-NMR (62.895 MHz, $CDCl_3$): 10.09 (Me); 10.49 (Me); 11.90 (Me); 30.82 (*Me*$_3$C); 44.94 (Me$_3$*C*); 74.78 (CH (Cp)); 77.62 (^{t}BuS*C*); 83.31 (Me*C* (Cp)); 83.40 (Me*C* (Cp)); 86.04 (Me*C* (Cp)).

Data of **3a**/**3b**: IR (KBr): 3072, 2957, 2897, 1655, 1472, 1456, 1377, 1360, 1290, 1169, 1032, 977, 836, 750, 696, 518, 457. EI-MS: 446 (100, $M^{+\bullet}$), 390, 334, 301, 299, 193, 162, 105. Anal. calc. for $C_{24}H_{38}FeS_2$ (893.1): C 64.55, H 8.58, S 14.36; found: C 64.68, H 8.51, S 14.41.

Synthesis of **3a** *by Reduction of the Corrresponding [Ni(mnt)$_2$]$^-$ Salt* **26**. [**3a**][Ni(mnt)$_2$] (**26**; 754 mg) was vigorously stirred in sodium dithionite soln./^{t}BuOMe until the black crystals dissolved. The red aq. soln. containing [Ni(mnt)$_2$]$^{2-}$ was separated and the org. phase dried ($MgSO_4$) and evaporated: 425 mg (99%) of **3a**. M.p. 134–136°. ^{1}H-NMR: *meso*/*rac* 94:6.

2,3,4-Trimethylcyclopent-2-en-1-ol (**9**) [47]. To a soln. of **7** (10 g, 80 mmol) in Et_2O (100 ml), $LiAlH_4$ (3.4 g, 90 mmol) was added in portions. The resulting mixture was stirred for 24 h at r.t. Then, 2N HCl was slowly added until the excess of $LiAlH_4$ was hydrolyzed. The org. phase was filtered over *Celite*, and the lithium and aluminium salts were washed with ^{t}BuOMe. The combined org. phase was evaporated and the residue distilled at 94°/4 mbar in a bulb-to-bulb distillation apparatus. 8.74 g (87%) of **9** *cis*/*trans ca*. 3:1. GC/EI-MS: 126 (20, $M^{+\bullet}$), 111, 43, 29, 15 (100).

1,1′,2,2′,3,3′-Hexamethylferrocene (**11**). At 1 atm/170° (bath) **9** (7.5 g, 59 mmol) was distilled. At this temp., trimethylcyclopentadiene distilled together with H_2O (boiling temp. 92°) directly into a cooled *Schlenk* tube (−78°), to prevent *Diels-Alder* dimerization. When the distillation was complete, pentane was added to the distillate and the soln. dried ($MgSO_4$) and evaporated at 0°. 5 g (47.8 mmol, 81%) of 1,2,3-trimethylcyclopenta-1,3-diene (**10**). This product was immediately cooled to −78°, mixed with THF (10 ml) and 2M LDA in THF/ethylbenzene (31 ml, 62 mmol), and stirred for 15 min. Anh. iron(II) chloride (4.6 g, 36 mmol) was added in one portion and the mixture allowed to warm to r.t. The resulting mixture was dissolved in ^{t}BuOMe and treated wtih 2N HCl and brine. The residue from the org. phase was chromatographed (silica gel, hexane): 2.4 g (30%) of **11**. IR (KBr): 3068, 2902, 1475, 1377, 1030, 802, 474. ^{1}H-NMR: 1.79 (*s*, 2 Me); 1.85 (*s*, 4 Me); 3.61 (*s*, 4 CH (Cp)). ^{13}C-NMR: 9.66 (Me); 12.19 (Me); 68.44 (CH (Cp)); 80.82 (Me*C*); 82.01 (Me*C*). EI-MS: 270 (100, $M^{+\bullet}$), 255, 160, 148, 135, 105, 91. Anal. calc. for $C_{16}H_{22}Fe$ (270.2): C 71.12, H 8.21; found: C 71.10, H 8.14.

rac-*1-Formyl-2,2′,3,3′,4,4′-hexamethylferrocene* (**12**). A mixture of **11** (2.4 g, 8.8 mmol), DMF (14 ml), and $POCl_3$ (2.4 ml, 26.4 mmol) was stirred overnight. A sat. NaOAc soln. was added and the resulting mixture stirred for an additional hour. The product was extracted with CH_2Cl_2 and chromatographed (silica gel, hexane/AcOEt 3:1): 1.65 g (63%) of **12**. M.p. 128°. IR (KBr): 3065, 2965, 2907, 1666, 1412, 1380, 1157, 1033, 844, 799, 744, 721, 684, 656, 612, 510, 470. ^{1}H-NMR: 1.69 (*s*, Me); 1.76 (*s*, Me); 1.77 (*s*, Me); 1.88 (*s*, Me); 1.94 (*s*, Me); 2.09 (*s*, Me); 3.65 (*d*, 1 CH (Cp)); 3.69 (*d*, 1 CH (Cp)); 4.25 (*s*, 1 CH (Cp)); 9.89 (*s*, CHO). ^{13}C-NMR: 194.54 (CHO): 87.89 (Me*C* (Cp)); 87.35 (Me*C* (Cp)); 84.39 (Me*C* (Cp)); 83.98 (Me*C* (Cp)); 83.29 (Me*C* (Cp)); 82.43 (Me*C* (Cp)); 75.02 (Me*C* (Cp)); 70.24 (CH (Cp)); 69.98 (CH (Cp)); 69.82 (CH (Cp)); 12.25 (Me); 11.73 (Me); 11.59 (Me); 10.25 (Me); 9.66 (Me); 9.17 (Me). EI-MS: 298 (100, $M^{+\bullet}$), 269, 255, 240, 163, 148, 107, 91, 79, 56. Anal. calc. for $C_{17}H_{22}FeO$ (298.2): C 68.47, H 7.44; found: C 68.33, H 7.42.

rac-*1-[(1,3-Benzodithiol-2-ylidene)methyl]-2,2′,3,3′,4,4′-hexamethylferrocene* (**5**). A soln. of dimethyl 1,3-benzodithiol-2-ylphosphonate [48–50] (**18a**; 106 mg, 0.404 mmol) in THF (15 ml) was mixed with 1M BuLi in hexane (0.26 ml, 0.416 mmol) at −78°. Then a soln. of **12** (120 mg, 0.404 mmol) in THF (5 ml) was added dropwise. After 1.5 h, the mixture was warmed to r.t., and a sat. NH_4Cl soln. (6 ml) and CH_2Cl_2 (35 ml) were

added. The org. phase was washed with H_2O, evaporated, and chromatographed (silica gel, hexane/AcOEt 10:1): 131 mg (75%) of **5**. M.p. 109°. IR (KBr): 3066, 2963, 2908, 1670, 1583, 1446, 435, 1397, 1374, 1293, 1258, 1124, 1030, 802, 731, 680, 640, 469. ^{1}H-NMR (300.13 MHz): 1.76 (*s*, Me); 1.84 (*s*, Me); 1.85 (*s*, Me); 1.87 (*s*, Me); 1.89 (*s*, Me); 1.99 (*s*, Me); 3.56 (*d*, *J* = 2.1, 1 CH (Cp)); 3.63 (*d*, *J* = 2.1, 1 CH (Cp)); 4.21 (*s*, 1 CH (Cp)); 6.16 (*s*, S_2C=C*H*); 7.3–7.0 (complex *m*, 4 arom. H). ^{13}C-NMR (75.47 MHz): 9.1 (Me); 10.0 (Me); 10.1 (Me); 11.5 (Me); 11.7 (Me); 12.3 (Me); 66.9 (CH (Cp)); 69.5 (CH (Cp)); 69.6 (CH (Cp)); 79.1 (CH–*C* (Cp)); 80.0 (Me*C* (Cp)); 81.1 (Me*C* (Cp)); 81.7 (Me*C* (Cp)); 82.1 (Me*C* (Cp)); 82.5 (Me*C* (Cp)); 82.7 (Me*C* (Cp)); 111.3 (S_2C=*C*H); 120.6 (arom. CH); 121.3 (arom. CH); 124.4 (S_2*C*=CH); 125.0 (arom. CH); 125.3 (arom. CH); 135.3 (arom. C–S); 136.9 (arom. C–S). EI-MS: 434 (100, $M^{+\bullet}$); 420, 303, 271, 237, 217, 196, 161, 119, 105. Anal. calc. for $C_{24}H_{26}FeS_2$ (434.4): C 66.35, H 6.28, S 14.76; found: C 66.58, H 6.28, S 14.55.

rac-*1-[1-(1,3-Benzodithiol-2-ylidene)-2-oxomethyl]-2,2′,3,3′,4,4′-hexamethylferrocene* (**13**). A mixture of **5** (138.4 mg, 0.318 mmol), $POCl_3$ (0.03 ml, 0.329 mmol), and DMF (1.5 ml, 19.5 mmol) was stirred overnight. The resulting dark mixture was cooled to 0° and mixed with a NaOAc soln. After 2 h, the product was extracted (CH_2Cl_2, 2N HCl, $NaHCO_3$, and brine), the org. phase evaporated, and the residue chromatographed (silica gel, hexane/AcOEt 10:1): 85 mg (58%) of **13**. M.p. 131°. IR (KBr): 3068, 2963, 2941, 2903, 2853, 1622, 1452, 1436, 1398, 1206, 1027, 737, 659, 576, 472. ^{1}H-NMR: 1.72 (*s*, Me); 1.78 (*s*, Me); 1.79 (*s*, Me); 1.82 (*s*, Me); 1.86 (*s*, Me); 1.90 (*s*, Me); 3.68 (*d*, *J* = 2.5, 1 CH (Cp)); 3.81 (*s*, 1 CH (Cp)); 3.83 (*d*, *J* = 2.5, 1 CH (Cp)); 7.6–7.2 (complex *m*, 4 arom. H); 10.06 (*s*, CHO). ^{13}C-NMR: 8.99 (Me); 9.63 (Me); 11.03 (Me); 11.36 (Me); 11.51 (Me); 12.15 (Me); 68.52 (CH (Cp)); 68.88 (CH (Cp)); 69.27 (CH (Cp)); 80.66 (Me*C* (Cp)); 81.54 (Me*C* (Cp)); 81.71 (Me*C* (Cp)); 81.91 (Me*C* (Cp)); 82.51 (2 Me*C* (Cp)); 117.396 (S_2C=*C*); 121.42 (arom. CH); 122.67 (arom. CH); 126.19 (arom. CH); 126.31 (arom. CH); 132.87 (arom. C–S); 138.81 (arom. C–S); 158.26 (S_2*C*=C); 87.97 (CHO). EI-MS: 462 (100, $M^{+\bullet}$), 355, 270. Anal. calc. for $C_{25}H_{26}FeOS_2$ (462.5): C 64.93, H 5.67; found: C 65.03, H 5.74.

rac-*1-[1,2-Bis(1,3-benzodithiol-2-ylidene)ethyl]-2,2′,3,3′,4,4′-hexamethylferrocene* (**14**). As described for **5**, with **18a** (111 mg, 0.42 mmol), THF (10 ml), 1.6M BuLi in hexane (0.28 ml, 0.45 mmol), and **13** (128 mg, 0.28 mmol): 146 mg (87%) of **14**, after chromatography (silica gel, hexane/AcOEt 20:1). ^{1}H-NMR: 1.70 (*s*, Me); 1.78 (*s*, Me); 1.79 (*s*, Me); 1.80 (*s*, Me); 1.86 (*s*, Me); 1.84 (*s*, Me); 3.77 (*d*, *J* = 2.2, 1 CH (Cp)); 3.94 (*d*, *J* = 2.2, 1 CH (Cp)); 4.03 (*s*, 1 CH (Cp)); 6.40 (*s*, S_2C=C–CH=CS_2); 7.3–7.0 (complex *m*, 8 arom. CH). ^{13}C-NMR: 9.00 (Me); 9.51 (Me); 11.36 (Me); 11.43 (Me); 11.62 (Me); 12.11 (Me); 67.66 (CH (Cp)); 68.58 (CH (Cp)); 69.40 (CH (Cp)); 80.93 (Me*C*); 81.29 (Me*C*); 81.74 (Me*C*); 82.27 (Me*C*); 82.49 (Me*C*); 83.92 (Me*C*); 116.6, 120.22 (S_2C=*C*–*C*H=CS_2); 121.23 (arom. CH); 121.36 (arom. CH); 121.66 (arom. CH); 125.17 (arom. CH); 125.25 (arom. CH); 125.39 (arom. CH); 125.85 (arom. CH); 126.64 (arom. CH); 130.43 (S_2*C*=C–CH=*C*S_2); 133.83 (arom. C–S); 135.51 (arom. C–S); 136.85 (arom. C–S); 137.26 (arom. C–S). EI-MS: 462 (100, $M^{+\bullet}$). 355, 270. Anal. calc. for $C_{32}H_{30}FeS_4$ (598.7): C 64.20, H 5.05; found: C 64.31, H 5.21.

1,1′-Diformyl-2,2′,3,3′,4,4′-hexamethylferrocene (mixture of diastereoisomers; **15**). A mixture of **11** (200 mg, 0.740 mmol), freshyl distilled TMEDA (0.28 ml, 1.87 mmol), and 1.6M BuLi in hexane (1.1 ml, 1.76 mmol) was stirred overnight in hexane (10 ml). The resulting orange soln. was slowly added dropwise to a soln. of DMF (0.13 ml, 1.69 mmol) in Et_2O (2 ml). After additional 20 min, 2N HCl (8 ml) was added. The red org. phase was evaporated and the residue chromatographed (silica gel, hexane/AcOEt 3:1): 6 mg (2.5%) of **15**. ^{1}H-NMR: 1.59 (*s*, 2 Me); 1.81 (*s*, 2 Me); 1.88 (*s*, 2 Me); 1.89 (*s*, 2 Me); 2.03 (*s*, 2 Me); 2.04 (*s*, 2 Me); 4.29 (*s*, 2 CH (Cp)); 4.31 (*s*, 2 CH (Cp)); 9.88 (*s*, 2 CHO); 9.91 (*s*, 2 CHO). IR (KBr): 3089, 2955, 2913, 1657, 1446, 1415, 1385, 1364, 1158, 1073, 1033, 829, 722, 651, 624, 510, 465.

1,1′,2,2′,3,3′-Hexamethyl-4,4′-trithioferrocene (four stereoisomers; **16**). To a mixture of **11** (200 mg, 0.739 mmol) and 1.6M BuLi in hexane (1 ml, 1.6 mmol), freshly distilled TMEDA (0.27 ml, 1.78 mmol) was added dropwise and the resulting mixture stirred overnight. The solvent ws evaporated and the residue dissolved in THF (2 ml). This soln. was transferred to a suspension of sulfur (145 mg, 4.53 mmol) in THF (10 ml). The resulting dark mixture was refluxed overnight and then evaporated and the residue chromatographed (silica gel, hexane): 9 mg (4%) of **16**. M.p. 114°. IR (KBr): 2966, 2987, 1635, 1470, 1442, 1374, 1298, 1123, 1025, 826, 815, 484, 473. ^{1}H-NMR: 4.17 (*s*, 2 CH (Cp)); 3.52 (*s*, 2 CH (Cp)); 3.48 (*s*, 2 CH (Cp)); 2.89 (*s*, 2 CH (Cp)); 1.81–1.1 (all Me). EI-MS: 364 (100, $M^{+\bullet}$), 331, 300, 258, 241, 209, 192, 182, 138, 105.

[(1,3-Benzodithiol-2-ylidene)methyl]ferrocene (**19a**). As described for **5** with **18a** (3.67 g, 14 mmol), THF (70 ml), 1.6M BuLi in hexane (8.75 ml, 14 mmol), and formylferrocene (**17**; 2 g, 9.3 mmol) in THF (50 ml): 3.5 g (quant.) of **19a**. M.p. 154°. IR (KBr): 3091, 1588, 1446, 1102, 1031, 807, 745, 503. ^{1}H-NMR: 4.21 (*s*, 5 CH (Cp)); 4.27 (*m*, *J* = 1.87, 2 CH (Cp)); 4.46 (*m*, *J* = 1.87, 2 CH (Cp)); 6.2 (*s*, S_2C=CH); 7.11–7.29 (complex *m*, 4 arom. CH). ^{13}C-NMR: 67.79 (CH (Cp)); 68.77 (CH (Cp)); 69.51 (CH (Cp)); 83.12 (CH–*C* (Cp)); 112.41 (S_2C=*C*H); 121.36 (arom. CH); 121.99 (arom. CH); 125.82 (arom. CH); 126.14 (arom. CH); 127.96

(S_2C=CH); 135.91 (arom. C–S); 137.35 (arom. C–S). EI-MS: 350 (100, $M^{+\cdot}$), 229, 197, 120. Anal. calc. for $C_{18}H_{14}FeS_2$ (434.4): C 61.72, H 4.03, S 18.31; found: C 61.47, H 4.25, S 18.04.

*[(5,6-Dihydro-1,3-dithiolo[4,5-*b*][1,4]dithiin-2-ylidene)methyl]ferrocene* (**19b**). As described for **5**, with dimethyl (5,6-dihydro-1,3-dithiolo[4,5-*b*][1,4]dithiin-2-yl)phosphonate [20][51][52] (**18b**; 848 mg, 2.8 mmol), THF (50 ml), 1.6M BuLi in hexane (1.75 ml, 2.8 mmol), and **17** (0.5 g, 2.3 mmol) in THF (25 ml): 0.89 g (98%) of **19b**, after chromatography (silica gel, hexane AcOEt 4:1). M.p. 160°. IR (KBr): 3090, 3000, 2976, 2909, 1583, 1287, 1104, 999, 810, 704, 646, 492, 464. ^{1}H-NMR: 3.32 (*s*, 2 CH_2); 4.16 (*s*, 5 CH (Cp)); 4.22 (*m*, *J* = 1.88, 2 CH (Cp)); 4.35 (*m*, *J* = 1.88, 2 CH (Cp)); 6.15 (*s*, S_2C=CH). ^{13}C-NMR: 30.09 (CH_2); 30.20 (CH_2); 67.71 (CH (Cp)); 68.88 (CH (Cp)); 69.5 (CH (Cp)); 82.73 (CH–*C* (Cp)); 111.29 (CS_2); 111.49 (CS_2); 113.17 (S_2C=*C*H); 125.46 (CS_2). EI-MS: 390 (100, $M^{+\cdot}$), 362, 269, 242. Anal. calc. for $C_{16}H_{14}FeS_4$ (390.4): C 49.23, H 3.61, S 32.85; found: C 49.28, H 3.66, S 32.67.

[1-(1,3-Benzodithiol-2-ylidene)-2-oxoethyl]ferrocene (**20a**). As described for **13**, with DMF (20 ml), $POCl_3$ (0.81 ml, 1.34 g, 8.7 mmol), **19a** (2.96 g, 8.4 mmol), and NaOAc soln. (4.75 ml, 1.5 g · ml^{-1}): 2.87 g (90%) of **20a**. Dark red crystals. M.p. 149°. IR (KBr): 1633, 1494, 1268, 1113, 1047, 1001, 737, 500. ^{1}H-NMR: 4.24 (*s*, 5 CH (Cp)); 4.41 (*m*, *J* = 1.86, 2 CH (Cp)); 4.58 (*m*, *J* = 1.87, 2 CH (Cp)); 7.28–7.36 (complex *m*, 2 arom. CH); 7.51–7.62 (complex *m*, 2 arom. CH); 9.96 (*s*, CHO). ^{13}C-NMR: 67.99 (CH (Cp)); 68.70 (CH (Cp)); 69.74 (CH (Cp)); 84.08 (CH(O)C–*C* (Cp)); 118.35 (S_2C=*C*); 121.96 (arom. CH); 123.02 (arom. CH); 126.82 (arom. CH); 126.87 (arom. CH); 133.75 (arom. C–S); 138.89 (arom. C–S); 155.25 (S_2C=C); 186.73 (CHO). EI-MS: (100, $M^{+\cdot}$), 313, 251, 197, 153. Anal. calc. for $C_{19}H_{14}FeOS_2$ (378.3): C 60.34, H 3.70; found: C 60.32, H 3.84.

*[1-(5,6-Dihydro-1,3-dithiolo[4,5-*b*][1,4]dithiin-2-ylidene)-2-oxoethyl]ferrocene* (**20b**). As described for **13**, with DMF (3 ml), oxalyl chloride (220 µl, 325 mg, 2.56 mmol), **19b** (500 mg, 1.28 mmol), and sat. NaOAc soln. (5 ml). 476 mg (89%) of **20b**, after recrystallization from 1,2-dichloroethane as thin orange needles. M.p. 240° (dec). IR (KBr): 3090, 2964, 2924, 2836, 1614, 2527, 1486, 1421, 1376, 1350, 1274, 1205, 1173, 1119, 1105, 1042, 998, 925, 892, 827, 809, 663, 598, 568, 504, 488, 476, 434. ^{1}H-NMR: 3.37 (*s*, SCH_2CH_2S); 4.20 (*s*, 5 CH (Cp)); 4.35 (*m*, *J* = 2.00, 2 CH (Cp)); 4.50 (*m*, *J* = 2.00 Hz, 2 CH (Cp)); 9.78 (*s*, CHO). ^{13}C-NMR (75.467 MHz): 28.6 (SCH_2); 28.8 (SCH_2); 66.7 (CH (Cp)); 67.9 (CH (Cp)); 69.0 (CH (Cp)); 76.9 (CH(O)C–*C* (Cp)); 83.3, 184.5 (CHO). EI-MS: 418 (100, $M^{+\cdot}$), 390, 325, 270, 242, 205, 121. Anal. calc. for $C_{17}H_{14}FeOS_4$ (418.4): C 48.80, H 3.37, S 30.66; found: C 48.76, H 3.45, S 30.54.

[1,2-Bis(1,3-benzodithiol-2-ylidene)ethyl]ferrocene (**21a**). As described for **5**, with **18a** (523 mg, 1.98 mmol), THF (70 ml) 1.6M BuLi in hexane (1.3 ml, 2.08 mmol), **20a** (506 mg, 1.32 mmol), and THF (50 ml): 556 mg (82%) of **21a**, after chromatography (silica gel, hexane/AcOEt 3:1) and recrystallization from hexane. M.p. 90°. IR (KBr): 3053, 2920, 1569, 1541, 1447, 1432, 1121, 1105, 1029, 1000, 818, 739, 496. ^{1}H-NMR: 4.24 (*s*, 5 CH (Cp)); 4.28 (*m*, *J* = 1.9, 2 CH (Cp)); 4.57 (*m*, *J* = 1.9, 2 CH (Cp)); 6.18 (*s*, S_2C=C–CH=CS_2); 7.05–7.32 (complex *m*, 8 arom. CH). ^{13}C-NMR: 67.83 (CH (Cp)); 68.69 (CH (Cp)); 69.67 (CH (Cp)); 84.19 (CH(=C)C–*C* (Cp)); 114.81 (S_2C=C–*C*H=CS_2); 119.84 (S_2C=C–CH=CS_2); 121.62 (arom. CH); 121.78 (arom. CH); 121.97 (arom. CH); 122.08 (arom. CH); 125.72 (arom. CH); 125.91 (arom. CH); 125,95 (arom. CH); 125,98 (arom. CH); 128.97 (S_2C=C); 135.96 (arom. CS); 136.7 (arom. C–S); 137.24 (arom. C–S); 137.31 (arom. C–S); 137.71 (S_2C=C). EI-MS: 514 (100, $M^{+\cdot}$), 359, 327, 253, 221. Anal. calc. for $C_{26}H_{18}FeS_4$ (514.5): C 60.69, H 3.53, S 24.93; found: C 60.98, H 3.93, S 23.91.

*[1-(1,3-Benzodithiol-2-ylidene)-2-(5,6-dihydro-1,3-dithiolo[4,5-*b*][1,4]dithiin-2-ylidene)ethyl]ferrocene* (**21b**). As described for **5**, with **18b** (600 mg, 1.98 mmol), THF (70 ml), 1.6M BuLi in hexane (1.3 ml, 2.08 mmol), **20a** (502 mg, 1.32 mmol), and THF (50 ml): 452 mg (62%) of **21b**, after chromatography (silica gel, hexane/AcOEt 4:1). M.p. 171°. IR (KBr): 3053, 2920, 1569, 1541, 1447, 1287, 1260, 1121, 1105, 1029, 1000, 818, 739, 496. ^{1}H-NMR: 3.29 (*s*, SCH_2CH_2S); 4.22 (*s*, 5 CH (Cp)); 4.27 (*m*, *J* = 1.9, 2 CH (Cp)); 4.53 (*m*, *J* = 1.9, 2 CH (Cp)); 6.16 (*s*, S_2C=C–CH=CS_2); 7.09–7.14 (complex *m*, 2 arom. CH); 7.25–7.31 (complex *m*, 2 arom. CH). ^{13}C-NMR: 30.12 (SCH_2); 67.97 (CH (Cp)); 68.69 (CH (Cp)); 69.66 (CH (Cp)); 84.12 (CH(=C)C–*C* (Cp)); 110.61, 112.95, 115.50, 119.51, 121.66 (arom. CH); 121.94 (arom. CH); 125.75 (arom. CH); 125.99 (arom. CH); 129.17, 134.49, 136.6, 137.64. EI-MS: 554 (100, $M^{+\cdot}$), 514, 438, 172, 108. Anal. calc. for $C_{24}H_{18}FeS_6$ (554.6): C 51.97, H 3.27, S 34.69; found: C 52.13, H 3.37, S 34.41.

*[1,2-Bis(5,6-dihydro-1,3-dithiolo[4,5-*b*][1,4]dithiin-2-ylidene)ethyl]ferrocene* (**21c**). As described for **5**, with **18b** (162 mg, 0.54 mmol), THF (15 ml), 1.6M BuLi in hexane (0.33 ml, 0.54 mmol), and **20b** (150 mg, 0.35 mmol): 150 mg (72%) of **21c**, after chromatography (silica gel, AcOEt/hexane/CH_2Cl_2 10:2:5). M.p. *ca.* 180° (dec.). IR (KBr): 3081, 2917, 1560, 1521, 1409, 1285, 1257, 1105, 1021, 1001, 917, 883, 819, 790, 679, 601, 493. ^{1}H-NMR: 3.30 (*s*, 4 H, SCH_2CH_2S); 3.34 (*s*, 4 H, SCH_2CH_2S); 4.20 (*s*, 5 CH (Cp)); 4.24 (*m*, *J* = 1.7, 2 CH (Cp)); 4.45 (*m*, *J* = 1.7, 2 CH (Cp)); 6.08 (*s*, S_2C=C–CH=CS_2). ^{13}C-NMR (75.467 MHz, 25°): 29.2 (SCH_2); 29.3

(SCH_2); 29.4 (SCH_2); 67.0 (CH (Cp)); 68.0 (CH (Cp)); 68.9 (CH (Cp)); 83.1 CH(=C)C–*C* (Cp)); 110.1, 118.8, 112.4, 114.2 (S_2C=C–*C*H=CS_2); 119.1, 125.9, 134.0. EI-MS: 594 (10, $M^{+\bullet}$), 566, 538, 446, 416, 403, 330, 300 (100), 150. Anal. calc. for $C_{22}H_{18}FeS_8$ (594.7): C 44.43, H 3.05; found: C 44.38, H 3.01.

*[2-(1,3-Benzodithiol-2-ylidene)-1-(5,6-dihydro-1,3-dithiolo[4,5-*b*][1,4]dithiin-2-ylidene)ethyl]ferrocene* (**21d**). As described for **5**, with **18a** (141 mg, 1.98 mmol), THF (15 ml), 1.6M BuLi in hexane (0.33 ml, 0.54 mmol), and **20b** (150 mg, 0.35 mmol): 75 mg (39%) of **21d**, after chromatography (silica gel, AcOEt/hexane/CH_2Cl_2 10:2:5). M.p. 109°. IR (KBr): 3088, 2918, 1571, 1551, 1508, 1447, 1432, 1410, 1287, 1260, 1121, 1105, 1030, 1000, 919, 884, 819, 742, 677, 604, 495. ^{1}H-NMR: 3.33 (*s*, SCH_2CH_2S); 4.22 (*s*, 5 CH (Cp)); 4.25 (*m*, *J* = 1.7, 2 CH (Cp)); 4.50 (*m*, *J* = 1.7, 2 CH (Cp)); 6.10 (*s*, S_2=C–CH=CS_2); 7.0–7.2 (complex *m*, arom. CH). ^{13}C-NMR (75.467 MHz): 29.2 (SCH_2); 29.3 (SCH_2); 67.0 (CH (Cp)); 68.0 (CH (Cp)); 68.9 (CH (Cp)); 83.1 (CH(=C)C–C (Cp)); 111.6, 112.4, 113.5 (S_2C=C–*C*H=CS_2); 119.4, 121.0 (arom. CH); 121.4 (arom. CH); 125.2 (arom. CH); 125.3 (arom. CH); 125.7, 135.2, 136.6, 136.7. EI-MS: 554 (20, $M^{+\bullet}$), 526, 419, 390, 270, 242, 205, 121 (100). Anal. calc. for $C_{24}H_{18}FeS_6$ (554.6): C 51.97, H 3.27; found: C 52.64, H 3.62.

1,1′-Bis[1-(1,3-benzodithiol-2-ylidene)-2-oxoethyl]ferrocene (**23a**). As described for **13**, with DMF (17 ml), $POCl_3$ (0.2 ml, 0.34 g, 2.22 mmol), 1,1′-bis[(1,3-benzodithiol-2-yliden)methyl]ferrocene [2] (**22a**; 0.567 g, 1.1 mmol), and a NaOAc soln. (17 ml, 3 g in 20 ml of H_2O): 0.44 g (71%) of **23a**, after recrystallization from 1,2-dichloroethane. IR (KBr): 3073, 2836, 1632, 1491, 1478, 1272, 1112, 740, 505. ^{1}H-NMR: 4.44 (*m*, *J* = 1.8, 4 CH (Cp)); 4.68 (*m*, *J* = 1.8, 4 CH (Cp)); 7.15–7.28 (complex *m*, 4 arom. CH); 7.42–7.54 (complex *m*, 4 arom. CH); 9.78 (*s*, 2 CHO). ^{13}C-NMR: 68.23 (CH (Cp)); 69.33 (CH (Cp)); 85.08 (CH(O)C–*C* (Cp)); 116.50 (S_2C=C); 121.47 (arom. CH); 122.46 (arom. CH); 126.24 (arom. CH); 126.31 (arom. CH); 138.35 (arom. C–S); 155.25 (arom. C–S); 185.24 (CHO). EI-MS: 570 (100, $M^{+\bullet}$), 313, 197. Anal. calc. for $C_{28}H_{18}FeO_2S_4$ (570.5): C 58.94, H 3.18, S 22.48; found: C 59.10, H 3.13, S 22.63.

1,1′-Bis[1,2-bis(1,3-benzodithiol-2-ylidene)ethyl]ferrocene (**6a**). As described for **5**, with **18a** (0.602 g, 2.6 mmol), THF (50 ml), 1.6M BuLi in hexane (1.44 ml, 2.30 mmol), and **23a** (0.44 g, 0.76 mmol) suspended in THF (150 ml): 0.56 g (88%) of **6a**, after chromatography (silica gel, CH_2Cl_2). M.p. 223° (dec.). IR (KBr): 3053, 2987, 1570, 1536, 1447, 1433, 1122, 735, 502, 476. ^{1}H-NMR: 4.37 (*m*, *J* = 1.7, 4 H, Cp); 4.62 (*m*, *J* = 1.7, 4 H, Cp); 6.17 (*s*, 2 S_2C=C–CH=CS_2); 6.99–7.21 (complex *m*, 16 arom. CH). ^{13}C-NMR: 68.62 (CH (Cp)); 69.44 (CH (Cp)); 84.76 (CH(=C)C–*C* (Cp)); 114.5 (S_2C=C–*C*H=C(S_2)); 118.43, 121.07 (arom. CH); 121.18 (arom. CH); 121.54 (arom. CH); 121.64 (arom. CH); 125.17 (arom. CH); 125.40 (arom. CH); 125.46 (arom. CH); 129.22, 135.55, 136.19, 136.65, 137.01, 137.28. EI-MS: 842 (20, $M^{+\bullet}$), 394, 303, 217 (100), 184, 110. Anal. calc. for $C_{42}H_{26}FeS_8$ (843.0): C 59.84, H 3.11; found: C 59.71, H 2.95.

*1,1′-Bis[1-(1,3-benzodithiol-2-ylidene)-2-(5,6-dihydro-1,3-dithiolo[4,5-*b*][1,4]dithiin-2-ylidene)ethyl]ferrocene* (**6b**). As described for **5**, with **18b** (0.625 g, 2.07 mmol), THF (50 ml), 1,6M BuLi in hexane (1.29 ml, 2.06 mmol) and **23a** (0.4 g, 0.69 mmol) suspended in THF (100 ml): 0.375 g (76%) of **6b**, after two recrystallizations, first from 1,2-dichloroethane, and second from benzene. M.p. 181° (dec.). IR (KBr): 3432, 2907, 1564, 1512, 1448, 1279, 1256, 1122, 1023, 952, 738, 494. ^{1}H-NMR: 3.29 (*s*, 2 SCH_2CH_2S); 4.35 (*m*, *J* = 1.7, 4 H, Cp); 4.57 (*m*, *J* = 1.7, 4 H, Cp); 6.13 (*s*, S_2C=C–CH=C(S_2)); 7.01–7.23 (complex *m*, 8 arom. CH). ^{13}C-NMR: 30.14 (SCH_2); 69.15 (CH (Cp)); 69.78 (CH (Cp)); 85.05 (CH(=C)C–*C* (Cp)); 110.71, 113.11, 115.66, 118.37, 121.54 (arom. CH); 121.96 (arom. CH); 125.63 (arom. CH); 125.83 (arom. CH); 129.85, 134.2, 136.51, 137.68. FAB-MS: 922 (100, $M^{+\bullet}$), 766, 391. Anal. calc. for $C_{38}H_{26}FeS_{12}$ (923.2): C 49.44, H 2.84; found: C 48.78, H 3.07.

Charge-Transfer Complexes with [M(mnt)$_2$]$^-$ (M = Ni, Pt): *General Procedure* (*GP*), *Exemplified by the Synthesis of* meso-*1,1′-Bis[(*tert*-butyl)thio]-2,2′,3,3′,4,4′-hexamethylferrocenium Bis[2,3-di(mercapto-*κ*S)but-2-enedinitrilato(2$^-$)]nickelate(1$^-$)* ([*meso*-Fe{η^5-C_5Me_3(S^{t}Bu)}$_2$][Ni(mnt)$_2$]; **26**). *meso*-Enriched **3a** (103 mg, 0.23 mmol; *meso*/*rac* 85:15) and ferrocenium bis[2,3-di(mercapto-*κS*)but-2-enedinitrilato(1–)]nickelate(1–) [$FeCp_2$][Ni(mnt)$_2$]; **24**; 104 mg, 0.20 mmol) were refluxed in MeCN. Then the mixture was evaporated and the residue recrystallized from AcOEt: 116 mg (64%) of **26**. Black needles. Single crystals were obtained by slow diffusion of hexane into a sat. soln. of the salt in CH_2Cl_2. IR (KBr): 3107, 2923, 2207, 1632, 1416, 1160, 1009, 855, 502. Anal. calc. for $C_{32}H_{38}FeN_4NiS_6$ (785.6): C 48.92, H 4.88, N 7.13; found: C 49.06, H 4.92, N 7.09.

meso-*1,1′-Bis[(*tert*-butyl)thio]-2,2′,3,3′,4,4′-hexamethylferrocenium Bis[2,3-di(mercapto-*κ*S)but-2-enedinitrilato(2–)]platinate(1–)* ([*meso*-Fe{η^5-C_5Me_3(S^{t}Bu)}$_2$][Pt(mnt)$_2$]; **27**). According to the *GP*, from ferrocenium bis[2,3-di(mercapto-*κS*)but-2-enedinitrilato(1–)]platinate(1–) ([$FeCp_2$][Pt(mnt)$_2$]; **25**; 110 mg, 0.17 mmol) and *meso*-enriched **3a** (74 mg, 0.17 mmol; *meso*/*rac* 94:6). 79 mg (52%) of **27**. Black powder. Single crystals were obtained by slow diffusion of Et_2O into a sat. soln. of the salt in CH_2Cl_2. IR (KBr): 3070, 2961, 2922, 2210, 1445, 1364, 1162, 1017, 878, 570, 527, 360, 212. Anal. calc. for $C_{32}H_{38}FeN_4PtS_6$ (922.0): C 41.69, H 4.15, N 6.08; found: C 41.78, H 4.32, N 6.08.

1,1′,2,2′,3,3′,4,4′-Octamethyl-5,5′-trithioferrocenium Bis[2,3-di(mercapto-κS)-but-2-enedinitrilato(2−)]nickelate(1−) ([Fe(η^5-$C_5Me_4S)_2$S][Ni(mnt)$_2$]; **28**). According to the *GP*, from [Fe{(η^5-$C_5Me_4S)_2$S}] (**4**; 100 mg, 0.25 mmol) and **24** (134 mg, 0.25 mmol): 131 mg (72%) of **28**. Dec. >260°. Single crystals were obtained by slow diffusion of ^{t}BuOME into a sat. soln. of the salt in MeCN. IR (KBr): 2959, 2917, 2207, 1448, 1379, 1160, 1019, 524, 501, 400, 367. Anal. calc. for $C_{26}H_{24}FeN_4NiS_7$ (731.5): C 42.69, H 3.31, N 7.66; found: C 42.67, H 3.11, N 7.55.

1,1′,2,2′,3,3′,4,4′-Octamethyl-5,5′-trithioferrocenium Bis[2,3-di(mercapto-κS)-but-2-enedinitrilato(2−)]platinate ([Fe(η^5-$C_5Me_4S)_2$S][Pt(mnt)$_2$]; **29**). According to the *GP*, from [Fe{(η^5-$C_5Me_4S)_2$S}] (**4**) (80 mg, 0.24 mmol) and **25** (157 mg, 0.24 mmol): 124 mg (63%) of **29**. Dec. >260°. IR (KBr): 2960, 2919, 2208, 1448, 1378, 1162, 1019, 524, 500, 384, 354, 328. Anal. calc. for $C_{26}H_{24}FeN_4PtS_7$ (867.9): C 35.98, H 2.79, N 6.46; found: C 36.04, H 2.90, N 6.44.

rac-*1-[(1,3-Benzodithiol-2-ylidene)methyl]-2,2′,3,3′-4,4′-hexamethylferrocenium Bis[2,3-di(mercapto-κS)but-2-enedinitrilato(2−)]nickelate(1−) 1,2-Dichloroethane Adduct* (**30**). According to the *GP*, from **5** (30 mg, 0.069 mmol) and **24** (36.2 mg, 0.69 mmol): 36 mg (60%) of **30**, after recrystallization from 1,2-dichloroethane/hexane. Black powder. Dec. >240°. Single crystals were obtained by slow diffusion of hexane into a sat. soln. of the salt in 1,2-dichloroethane. IR (KBr): 1916, 2206, 1566, 1528, 1381, 1340, 1159, 1019, 946, 832, 805, 734, 678, 641, 518, 501, 366. Anal. calc. for $C_{34}H_{30}Cl_2FeN_4NiS_6$ (872.5): C 46.81, H 3.47, N 6.42; found: C 46.91, H 3.17, N 6.40.

1,1′Bis[1,2-bis(1,3-benzodithiol-2-ylidene)ethyl]ferrocenium Bis[2,3-di(mercapto-κS)but-2-enedinitrilato-(2−)]nickelate(1−) (**31**). According to the *GP*, from **6a** (50 mg, 0.059 mmol) and **24** (31 mg, 0.059 mmol) in 1,2-dichloroethane (5 ml) and MeCN (3 ml) by slow diffusion of hexane into this filtered soln. 32 mg (45%) of **31**. Very thin black needles. IR (KBr): 2206, 1569, 1539, 1473, 1453, 1435, 1377, 1291, 1203, 1159, 1120, 1055, 833, 740, 678, 631, 465. Anal. calc. for $C_{50}H_{26}FeN_4NiS_{12}$ (1182.1): C 50.80, H 2.22, N 4.74; found: C 51.29, H 2.18, N 4.78.

1,1′-Bis[1,2-bis(1,3-benzodithiol-2-ylidene)ethyl]ferrocenium Bis[2,3-di(mercapto-κS)but-2-enedinitrilato-(2−)]nickelate(1−) 1,2-Dichloroethane Adduct (**31a**). According to the *GP*, from **6a** (30 mg, 0.042 mmol) and **24** (23 mg, 0.042 mmol) in a minimal amount of 1,2-dichloroethane. Single crystals were obtained by slow diffusion of hexane into this filtered soln.: 23 mg (43%) of **31a** as black plates, together with 22 mg (44%) of **31** as very thin needles. **31a**: IR (Kbr): strong absorption down to 3000, 2204, 1567, 1472, 1401, 1368, 1268, 1207, 1120, 1060, 939, 905, 838, 800, 743, 706, 679, 457. Anal. calc. for $C_{52}H_{30}Cl_2FeN_4NiS_{12}$ (1281.0): C 48.76, H 2.36, N 4.37, S 30.04; found: C 48.95, H 2.58, N 4.39, S 29.76.

1,1′-Bis[1,2-bis(1,3-benzodithiol-2-ylidene)ethyl]ferrocenium Bis[2,3-di(mercapto-κS)but-2-enedinitrilato-(2−)]platinate(1−) (**32**). According to the *GP*, from **6a** (50 mg, 0.06 mmol) and **25** (40 mg, 0.06 mmol) in a minimal amount of 1,2-dichloroethane. The product was obtained by slow diffusion of ^{t}BuOMe into this filtered soln. and recrystallization from 1,2-dichloroethane: 13 mg (27%) of **32**. IR (KBr): 2206, 1567, 1534, 1471, 1453, 1434, 1405, 1372, 1276, 1203, 1162, 1118, 1042, 907, 821, 737, 678, 463. Anal. calc. for $C_{50}H_{26}FeN_4PtS_{12}$ (1318.4): C 45.55, H 1.99, N 4.25, S 29.18; found: C 45.67, H 1.86, N 4.33, S 28.99.

1,1′-Bis[1-(1,3-benzodithiol-2-ylidene)-2-(5,6-dihydro-1,3-dithiolo[4,5-b][1,4]dithiin-2-yliden)ethyl]ferrocenium Bis[2,3-di(mercapto-κS)but-2-enedinitrilato(2−)]nickelate(1−) (**33**). According to the *GP*, from **6b** (30 mg, 0.042 mmol) and **24** (23 mg, 0.042 mmol) in a minimal amount of 1,2-dichloroethane. The product was obtained by slow diffusion of ^{t}BuOMe into this filtered soln. and recrystallization from 1,2-dichloroethane: 14 mg (31%) of **33**. IR (KBr): 2205, 1420, 1378, 1271, 1200, 1113, 905, 796, 745, 679, 466. Anal. calc. for $C_{46}H_{26}FeN_4NiS_{16}$ (1262.3): C 43.77, H 2.08, N 4.44; found: C 43.75, H 2.37, N 4.53.

X-Ray Crystallographic Study of **6a**,**b**, **21c**,**d**, **23a**, **26**–**28**, **30**, and **31a**. Suitable crystals for an X-ray analysis of all of these compounds were obtained by slow diffusion of an apolar solvent (^{t}BuOMe or hexane) in a sat. soln. of the compounds in a polar solvent (CH_2Cl_2, 1,2-dichloroethane or MeCN). Selected crystallographic and relevant data collection parameters are listed in *Table 2*. Data were measured at r.t. (293(2) K) with variable scan speed to ensure constant statistical precision on the collected intensities. One standard reflection was measured every 120 reflections, and no significant variation was detected. The structures were solved by direct or *Patterson* methods and refined by full-matrix least squares with anisotropic displacement parameters for all non-H-atoms. The contribution of the H-atoms in their idealized position (riding model with fixed isotropic U = 0.080 Å^2) was taken into account but not refined. All calculations were carried out with the *Siemens* SHELX93 (VMS) system. Crystallographic data (excluding structure factors) for the structures reported in this paper have been deposited with the *Cambridge Crystallographic Data Centre* as supplementary publication no. CCDC 112672 to CCDC 112681. Copies of the data can be obtained free of charge on application to CCDC, 12 Union Road, Cambridge CB2 1EZ, UK (fax: (+44) 1223 336-033; e-mail: deposit@ccdc.cam.ac.uk).

Magnetic Measurements. The magnetic susceptibility χ of the charge-transfer complexes **26**–**30** and **31a** was measured in the temp. range of 2–300 K in an external variable magnetic field, by means of a *Quantum-Design* superconducting quantum interference device (SQUID) magnetometer. The polycrystalline samples were mounted in a sample-holder tube made of quartz glass in order to keep the magnetic background as low as possible. Routine corrections for the sample holder were applied.

S.Z. is grateful to the *Swiss National Science Foundation* for financial support (Grant 20-41974.94).

REFERENCES

[1] S. Zürcher, V. Gramlich, D. von Arx, A. Togni, *Inorg. Chem*. **1998**, *37*, 4015.
[2] M. Hobi, G. Rihs, G. Rist, A. Albinati, P. Zanello, D. Zech, H. Keller, A. Togni, *Organometallics* **1994**, *13*, 1224.
[3] M. Hobi, S. Zürcher, V. Gramlich, U. Burckhardt, C. Mensing, M. Spahr, A. Togni, *Organometallics* **1996**, *15*, 5342.
[4] M. Hobi, O. Ruppert, V. Gramlich, A. Togni, *Organometallics* **1997**, *16*, 1384.
[5] S. Zürcher, J. Petrig, V. Gramlich, M. Wörle, C. Mensing, D. von Arx, A. Togni, *Organometallics* **1999**, *18*, in press.
[6] M. Hobi, 'Ferrocene als Donoren in Charge-Transfer-Komplexen', Thesis No. 12184, ETH, Zürich, 1997.
[7] S. Zürcher, 'Ferrocenhaltige molekulare Materialien', Thesis No. 12895, ETH, Zürich, 1998.
[8] R. Broussier, S. Ninoreille, C. Legrand, B. Gautheron, *J. Organomet. Chem*. **1997**, *532*, 55.
[9] R. Broussier, S. Ninoreille, C. Bourdon, O. Blacque, C. Ninoreille, M. M. Kubicki, B. Gautheron, *J. Organomet. Chem.* **1998**, *561*, 85.
[10] T. Mukaiyama, K. Saigo, *Chem. Lett*. **1973**, 479.
[11] F. Akiyama, *Bull. Chem. Soc. Jpn*. **1977**, *50*, 936.
[12] A. Moore, P. J. Skabara, M. R. Bryce, A. S. Batsanov, J. A. K. Howard, S. T. K. Daley, *J. Chem. Soc., Chem. Commun*. **1993**, 417.
[13] M. Schlosser, *Pure Appl. Chem.* **1988**, *60*, 1627.
[14] C. Zou, M. S. Wrighton, *J. Am. Chem. Soc*. **1990**, *112*, 7578.
[15] S. Barlow, V. J. Murphy, J. S. O. Evans, D. O' Hare, *Organometallics* **1995**, *14*, 3461.
[16] S. Barlow, D. O' Hare, *Organometallics* **1996**, *15*, 3885.
[17] H. T. Kruse, M. V. Lakshmikantham, M. P. Cava, J. Becher, *J. Chem. Soc., Perkin Trans.* **1991**, 2873.
[18] Y. Misaki, N. Higuchi, H. Fujiwara, T. Yamabe, T. Mori, H. Mori, S. Tanaka, *Angew. Chem*. **1995**, *107*, 1340.
[19] M. R. Bryce, *J. Chem. Soc., Chem. Commun.* **1983**, 4.
[20] A. J. Moore, M. R. Bryce, *Synthesis* **1991**, 26.
[21] A. J. Moore, M. R. Bryce, D. J. Ando, M. B. Hursthouse, *J. Chem. Soc., Chem. Commun.* **1991**, 320.
[22] Z. Yoshida, T. Kawase, H. Awaji, S. Yoneda, *Tetrahedron Lett*. **1983**, *24*, 3473.
[23] Y. Misaki, T. Matsumura, T. Sugimoto, Z. Yoshida, *Tetrahedron Lett*. **1989**, *30*, 5289.
[24] R. P. Clausen, J. Becher, *Tetrahedron* **1996**, *52*, 3171.
[25] T. K. Hansen, M. V. Lakshmikantham, M. P. Cava, R. M. Metzger, J. Becher, *J. Org. Chem*. **1991**, *56*, 2720.
[26] M. A. Coffin, M. B. Bryce, A. S. Batsanov, J. A. K. Howard, *J. Chem. Soc., Chem. Commun.* **1993**, 552.
[27] P. Cassoux, L. Valade, in 'Inorganic Materials', Eds. D. W. Bruce and D. O' Hare, Wiley, Chichester, 1992, pp. 1–58.
[28] C. J. Fritchie, *Acta Crystallogr*. **1966**, *20*, 107.
[29] A. Kobayashi, Y. Sasaki, *Bull. Chem. Soc. Jpn.* **1977**, *50*, 2650.
[30] J. S. Miller, J. C. Calabrese, A. J. Epstein, *Inorg. Chem.* **1989**, *28*, 4230.
[31] J. F. Weiher, L. R. Melby, R. E. Benson, *J. Am. Chem. Soc*. **1964**, *86*, 4329.
[32] P. I. Clemenson, A. E. Underhill, M. B. Hursthouse, R. L. Short, *J. Chem. Soc., Dalton Trans.* **1989**, 61.
[33] B. N. Figgis, R. L. Martin, *J. Chem. Soc*. **1956**, 3837.
[34] B. L. Ramakrishna, *Inorg. Chim. Acta* **1986**, *114*, 31.
[35] M. Fettouhi, L. Ouahab, M. Hagiwara, E. Codjovi, O. Kahn, H. Constant-Machado, F. Varret, *Inorg. Chem*. **1995**, *34*, 4152.
[36] W. E. Broderick, J. A. Thompson, M. R. Godfrey, M. Sabat, B. M. Hoffman, *J. Am. Chem. Soc*. **1989**, *111*, 7656.
[37] J. A. McCleverty, *Prog. Inorg. Chem*. **1968**, *10*, 50–215.

[38] J. S. Miller, J. C. Calabrese, A. J. Epstein, R. W. Bigelow, J. H. Zhang, W. M. Reiff, *J. Chem. Soc., Chem. Commun*. **1986**, 1026.
[39] W. E. Broderick, D. M. Eichhorn, X. Liu, P. J. Toscano, S. M. Owens, B. M. Hoffman, *J. Am. Chem. Soc*. **1995**, *117*, 3641.
[40] W. E. Broderick, J. A. Thompson, E. P. Day, B. M. Hoffman, *Science (Washington, D.C.)* **1990**, *249*, 401.
[41] W. E. Broderick, B. M. Hoffman, *J. Am. Chem. Soc*. **1991**, *113*, 6334.
[42] J. M. Conia, M.-L. Leriverend, *Bull. Soc. Chim. Fr.* **1970**, 2981.
[43] J. M. Conia, M.-L. Leriverend, *Bull. Soc. Chim. Fr.* **1970**, 2992.
[44] C. M. Fendrick, L. D. Schertz, V. W. Day, T. J. Marks, *Organometallics* **1988**, *7*, 1828.
[45] D. Feitler, G. M. Whitesites, *Inorg. Chem.* **1976**, *15*, 466.
[46] J. R. Sowa, R. J. Angelici, *J. Am. Chem. Soc*. **1991**, *113*, 2537.
[47] V. A. Mironov, E. V. Sobolev, A. N. Elizarova, *Tetrahedron* **1963**, 1939.
[48] J. Nakayama, *J. Chem. Soc., Chem. Commun*. **1975**, 38.
[49] I. Degani, R. Fochi, *J. Chem. Soc., Chem. Commun*. **1976**, 471.
[50] K. Ishikawa, N. Inamoto, K. Akiba, *Bull. Chem. Soc. Jpn*. **1978**, *51*, 2674.
[51] K. S. Varma, A. Bury, N. J. Harris, E. Underhill, *Synthesis* **1987**, 837.
[52] H. J. Sieler, R. Kirmse, E. Hoyer, G. Steimecke, *Phosphorus, Sulfur Relat. Elem.* **1979**, *7*, 49.

Received May 4, 1999